Inorganic Chemistry

Article

pubs.acs.org/IC

Synthesis, Crystal Structures, Magnetic Properties, and Theoretical Investigation of a New Series of Ni^{II}–Ln^{III}–W^{V} Heterotrimetallics: Understanding the SMM Behavior of Mixed Polynuclear Complexes

Veacheslav Vieru,[†] Traian D. Pasatoiu,[‡] Liviu Ungur,[†,§] Elizaveta Suturina,[†,∥] Augustin M. Madalan,[‡] Carine Duhayon,[⊥,#] Jean-Pascal Sutter,[⊥,#] Marius Andruh,*[,‡] and Liviu F. Chibotaru*[,†]

[†]Theory of Nanomaterials Group, Katholieke Universiteit Leuven, Celestijnenlaan 200F, 3001 Heverlee, Belgium

[‡]Inorganic Chemistry Laboratory, Faculty of Chemistry, University of Bucharest, Strada Dumbrava Rosie 23, 020464 Bucharest Romania

[§]Theoretical Chemistry, Lund University, Getingevagen 60, 22241, Lund, Sweden

[∥]Novosibirsk State University, Pirogova 2, 630090, Novosibirsk, Russia

[⊥]LCC (Laboratoire de Chimie de Coordination), CNRS, 205, route de Narbonne, F-31077 Toulouse, France

[#]UPS, INPT, LCC, Université de Toulouse, F-31077 Toulouse, France

Supporting Information

ABSTRACT: The polynuclear compounds containing anisotropic metal ions often exhibit efficient barriers for blocking of magnetization at fairly arbitrary geometries. However, at variance with mononuclear complexes, which usually become single-molecule magnets (SMM) under the sole requirement of a highly axial crystal field at the metal ion, the factors influencing the SMM behavior in polynuclear complexes, especially, with weakly axial magnetic ions, still remain largely unrevealed. As an attempt to clarify these conditions, we present here the synthesis, crystal structures, magnetic behavior, and *ab initio* calculations for a new series of Ni^{II}–Ln^{III}–W^{V} trimetallics, $[(CN)_7W(CN)Ni(H_2O)(valpn)Ln(H_2O)_4]\cdot H_2O$ (Ln = Y **1**, Eu **2**, Gd **3**, Tb **4**, Dy **5**, Lu **6**). The surprising finding is the absence of the magnetic blockage even for compounds involving strongly anisotropic Dy^{III} and Tb^{III} metal ions. This is well explained by *ab initio* calculations showing relatively large transversal components of the *g*-tensor in the ground exchange Kramers doublets of **1** and **4** and large intrinsic tunneling gaps in the ground exchange doublets of **3** and **5**. In order to get more insight into this behavior, another series of earlier reported compounds with the same trinuclear $[W^{V}Ni^{II}Ln^{III}]$ core structure, $[(CN)_7W(CN)Ni(dmf)(valdmpn)Ln(dmf)_4]\cdot H_2O$ (Ln = Gd^{III} **7**, Tb^{III} **8a**, Dy^{III} **9**, Ho^{III} **10**), $[(CN)_7W(CN)Ni(H_2O)$-$(valdmpn)Tb(dmf)_{2.5}(H_2O)_{1.5}]\cdot H_2O\cdot 0.5dmf$ **8b**, and $[(CN)_7W(CN)Ni(H_2O)(valdmpn)Er(dmf)_3(H_2O)_1]\cdot H_2O\cdot 0.5dmf$ **11**, has been also investigated theoretically. In this series, only **8b** exhibits SMM behavior which is confirmed by the present *ab initio* calculations. An important feature for the entire series is the strong ferromagnetic coupling between Ni(II) and W(V), which is due to an almost perfect trigonal dodecahedron geometry of the octacyano wolframate fragment. The reason why only **8b** is an SMM is explained by positive zero-field splitting on the nickel site, precluding magnetization blocking in complexes with fewer axial Ln ions. Further analysis has shown that, in the absence of ZFS on Ni ion, all compounds in the two series (except those containing Y and Gd) would be SMMs. The same situation arises for perfectly axial ZFS on Ni(II) with the main anisotropy axis parallel to the main magnetic axis of Ln(III) ions. In all other cases the ZFS on Ni(II) will worsen the SMM properties. The general conclusion is that the design of efficient SMMs on the basis of such complexes should involve isotropic or weekly anisotropic metal ions, such as Mn(II), Fe(III), etc., along with strongly axial lanthanides.

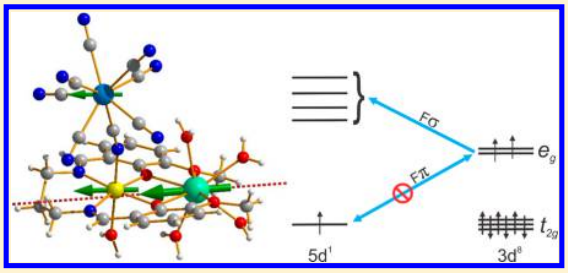

INTRODUCTION

Researchers' interest toward the field of molecular magnetism has increased considerably after the discovery of the first single-molecule magnet (SMM), $Mn_{12}(acac)$.[1] SMMs are currently regarded as promising materials for future storage devices and spintronics.[1,2] Early studies have indicated that the blocking barrier of magnetization depends on the total spin, the axial zero-field splitting (ZFS) parameter, and the total spin as $U_{eff} \sim |D|S^2$.[3] This is, first of all, the case of "classical" SMMs based on transition metals, such as $Mn_{12}(acac)$,[1] Fe_8,[4a] Mn_6,[4b] and others. After the first report on a single-ion lanthanide SMM, the double-decker Tb(III) phthalocyanide complex,[5] an intensive study of lanthanide based SMMs has begun, as they have been found to possess higher blocking barriers of magnetization.[6] This is entirely due to a different origin of

Received: July 15, 2016
Published: November 18, 2016

DOI: 10.1021/acs.inorgchem.6b01669
Inorg. Chem. 2016, 55, 12158−12171

relaxation barriers in lanthanide compounds. While in Mn_{12}(acac) the barrier is of exchange type, i.e., arising from the ZFS of the ground exchange multiplet S of the complex,[3] in single-ion lanthanides it arises from the crystal-field splitting of the ground atomic J multiplet.[5] Usually, this splitting arises in the form of separated doublets and the relaxation path goes via the first, second, or even third excited doublet.[7] As it was shown in previous studies, the key feature for the Ln^{III} ion to be good SMMs is the axiality of its ground and low-lying excited doublets.[8]

Interesting magnetic behavior has also been found in mixed transition metal−lanthanide complexes. In these compounds, the combination of the above factors will influence their ability to show SMM properties. Given the complexity of magnetic interaction in such systems, it is not possible to foresee a priori their blocking properties. Furthermore, the design of heterometallic complexes requires the development of an appropriate synthetic strategy. The synthetic task becomes more difficult when three different metal ions have to be gathered within the same molecular entity.

So far, the number of heterotrimetallic complexes, with all metal ions paramagnetic, is not large. The very first 3d−3d′−3d″ heterotrimetallic complexes, obtained in a rational way, were reported by Chaudhuri et al.[9] Their synthetic strategy is based upon unsymmetrical bicompartmental Schiff-base oxime ligands, which encapsulate two different metal ions, M_B and M_C. The preformed bimetallic oximate can further act as a ligand toward the third metal ion, M_A, whose coordination sphere is partially blocked by a capping ligand, tmtacn (1,4,7-trimethyl-1,4,7-triazacyclononane). Another rational synthetic approach is based on stable cationic 3d−3d′ heterobimetallic complexes, which are obtained employing dissymmetric macrocyclic compartmental ligands.[10] The self-assembly processes involving these binuclear species and anionic complexes, containing the third metal ion and potentially bridging groups (cyanide, oxalate), lead to the desired compounds. Following this route, several 3d−3d′−3d″ complexes have been obtained.[11] The one-pot procedures, which are rather serendipitous, can also generate heterotrimetallic complexes. For example, the reaction between copper powder, cobalt and nickel chlorides and 2-(dimethylamino)ethanol afforded alkoxo-bridged pentanuclear $[Cu_2^{II}Co^{II}Ni_2^{II}]$ complex].[12]

More numerous are heterotrimetallic complexes containing two different d metal ions and a lanthanide (3d−3d′−4f; 3d−4d−4f; 3d−5d−4f). A straightforward route leading to such systems employs preformed bi- or trinuclear 3d−4f complexes, which interact with an anionic metalloligand ($[M(CN)_6]^{3-}$, M = Fe^{III}, Cr^{III}; $[M(CN)_8]^{3-}$, M = Mo^{V}, W^{V}).[13,14] The bi- or trinuclear 3d−4f tectons are readily obtained using side-off compartmental Schiff-base ligands derived from *o*-vanillin.[13,14] Other useful trinuclear $\{M^{II}Ln^{III}M^{II}\}$ tectons (M = Co, Cu, Ni) are obtained using 2,6-di(acetoacetyl)pyridine as a ligand. A very interesting 3-D coordination polymer, showing spontaneous magnetization below T_c = 15.4 K, has been constructed from $\{Co^{II}Ln^{III}Co^{II}\}$ nodes and $[Cr(CN)_6]^{3-}$ spacers, which connect the cobalt ions from adjacent nodes.[15]

The design of heterotrimetallic complexes in itself remains a simple synthetic exercise if the third metal ion does not bring a new property or if it does not interact in a constructive way with the other metal ions. Within this line, it has been shown that, when paramagnetic complexes are employed as metalloligands, it is possible to connect SMMs, resulting in SCMs (single chain magnets).[13e,14] In order to observe the slow relaxation of the magnetization, which is characteristic for SMMs and SCMs, various metal ions exhibiting strong Ising magnetic anisotropy are commonly employed (Tb^{III}, Dy^{III}, Ho^{III}, Co^{II}, etc.). The analysis of the crystal structures of the heterotrimetallic complexes obtained from Cu^{II}−Ln^{III} nodes and polycyanido metalloligands shows that the metalloligand coordinates frequently into the apical position of the Cu^{II} ion. This means that the exchange interaction between Cu^{II} and the other metal ion is very weak. The problem can be solved by replacing Cu^{II} with Ni^{II}. Indeed, a rational way in constructing high spin heterotrimetallics was developed and consists of the assembling $[Ni^{II}Ln^{III}]^{3+}$ and $[W(CN)_8]^{3-}$ ions.[16] Two series of discrete heterotrimetallic complexes were obtained, depending on the nature of the solvent used: neutral trinuclear $[Ni^{II}Ln^{III}W^{V}]$ species, starting from $[(valdmpn)Ni(H_2O)_2Ln(O_2NO)_3]$ and $(NHBu_3)_3[W(CN)_8]$ through slow diffusion of tetrahydrofuran (thf) into the dimethylformamide (dmf) solution of the two precursors;[16a] neutral hexanuclear $[\{Ni^{II}Ln^{III}\}_2\{W^{V}\}_2]$ species, by reacting the two precursors, $[(valdmpn)Ni(H_2O)_2Ln(O_2NO)_3]$ and $Cs_3[W(CN)_8]$, in aqueous solution ($valdmpn^{2-}$ stands for the dianion of the Schiff-base resulting from the condensation of *o*-vanillin with 2,2-dimethyl-1,3-propanediamine).[16b] Within the trinuclear complexes, the metalloligand interacts solely with Ni^{II} ions. Previous works showed that Ni^{II}−W^{V} and Ni^{II}−Gd^{III} exchange interactions, in the corresponding bimetallic complexes, are ferromagnetic.[17,18] Consequently, the two exchange pathways within the $[W^{V}Ni^{II}Gd^{III}]$ trinuclear complex must be ferromagnetic. The magnetic measurements confirmed indeed these expectations, the ground state being S = 5. When Gd^{III} is replaced by the anisotropic Tb^{III} ion, the $[(CN)_7W(CN)Ni(H_2O)(valdmpn)Tb(dmf)_{2.5}(H_2O)_{1.5}]\cdot H_2O\cdot 0.5dmf$ complex behaves as an SMM.[16a] In other words, by combining three different ions, two important conditions for obtaining SMMs are easily fulfilled: a high spin, resulting from ferromagnetic interactions between the metal ions, and a strong magnetic anisotropy.

We have previously proved the existence of a ferromagnetic interaction between Ni^{II} and Gd^{III} or Ni^{II} and highly anisotropic Ln^{III} ions such as Tb^{III}, Dy^{III}, or Ho^{III} in $[Ni^{II}(valpn)Ln^{III}]$ heterodinuclear complexes ($valpn^{2-}$ represents the dianion of the Schiff base resulting from *o*-vanillin and 1,3-propanediamine in 2:1 molar ratio) and an SMM behavior for Tb^{III} and Dy^{III} derivatives.[18] Using $[Ni^{II}(valpn)Ln^{III}]$ building blocks we have obtained and characterized various systems, ranging from discrete to 1-D species.[19]

In this paper, we report on a new series of $[W^{V}Ni^{II}Ln^{III}]$ complexes with the general formula $[(CN)_7W(CN)Ni(H_2O)(valpn)Ln(H_2O)_4]\cdot H_2O$ (Ln = Y **1**, Eu **2**, Gd **3**, Tb **4**, Dy **5**, Lu **6**). Compounds **2**−**6** belong to a class of heterospin complexes which is now expanding: heteropolynuclear complexes containing three different metal ions, all paramagnetic.[14,16] The surprising finding, however, is the absence of the magnetic blockage even for compounds involving strongly anisotropic Dy^{III} and Tb^{III} metal ions. To understand this situation, **1**, **3**, **4**, and **5** complexes have been theoretically investigated by means of *ab initio* calculations. In order to get more insight into this behavior, another series of earlier reported compounds,[16a] with the same trinuclear $[W^{V}Ni^{II}Ln^{III}]$ core structure, $[(CN)_7W(CN)Ni(dmf)(valdmpn)Ln(dmf)_4]\cdot H_2O$ (Ln = Gd^{III} **7**, Tb^{III} **8a**, Dy^{III} **9**, Ho^{III} **10**), $[(CN)_7W(CN)Ni(H_2O)(valdmpn)Tb(dmf)_{2.5}(H_2O)_{1.5}]\cdot H_2O\cdot 0.5dmf$ **8b**, and $[(CN)_7W(CN)Ni$-

DOI: 10.1021/acs.inorgchem.6b01669
Inorg. Chem. 2016, 55, 12158−12171

$(H_2O)(valdmpn)Er(dmf)_3(H_2O)_1]\cdot H_2O\cdot 0.5dmf$ **11**, has been also investigated theoretically. In this series, only **8b** exhibits SMM behavior,[16a] which is confirmed by the present *ab initio* calculations. The reason why **8b** is the only slowly relaxing compound from the investigated large series is elucidated. The theoretical analysis allows the establishing of general rules for the design of efficient SMMs in this class of complexes.

EXPERIMENTAL SECTION

General Procedures and Materials. The chemicals used, i.e., *o*-vanillin, 1,3-diaminopropane, $Ni(NO_3)_2\cdot 6H_2O$, $Ln(NO_3)_3\cdot xH_2O$, and all the solvents (THF, acetonitrile), were of reagent grade and were purchased from commercial sources. $Cs_3[W(CN)_8]$ was obtained as indicated in the literature.[20]

The first step of the synthetic strategy consists of the formation of the heterodinuclear $[Ni^{II}(valpn)Ln^{III}]$ building blocks we have previously described.[18] In order to get heterotrimetallic $[Ni^{II}Ln^{III}W^{V}]$ systems, heterodinuclear $[Ni^{II}(valpn)Ln^{III}]$ complexes and $Cs_3[W^{V}(CN)_8]^{3-}$ react as indicated in Scheme 1.

Scheme 1. Synthesis of the Heterotrinuclear $[Ni^{II}Ln^{III}W^{V}]$ Systems

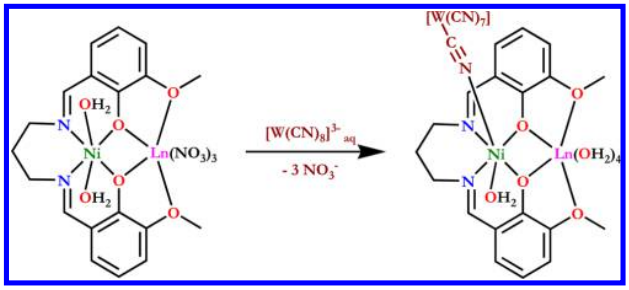

The reaction is done in tubes by slow diffusion of the reagents. The inferior layer was obtained by dissolving 0.1 mmol of $Cs_3[W^{V}(CN)_8]$ in 10 mL of water, while the upper one resulted by dissolving 0.1 mmol of the corresponding heterodinuclear $[Ni^{II}(valpn)Ln^{III}]$ complex in 10 mL of acetonitrile. The interface between these two solutions was made from 20 mL of a 1:1 water−acetone mixture. Crystals of the desired compounds, dark-green in color, were obtained after 1−2 days.

Crystallography. X-ray diffraction data for crystals of compounds **1**, **2**, **4**, **5**, and **6** were collected at 293 K on an IPDS II STOE diffractometer using a graphite-monochromated Mo Kα radiation source (λ = 0.71073 Å). For compound **3** diffraction data were collected at 180 K on an Apex2 Bruker diffractometer using a graphite-monochromated Mo Kα radiation source (λ = 0.71073 Å) and equipped with Oxford Cryosystems Cryostream Cooler devices. Multiscan absorption corrections were applied. Structures were solved by direct methods and refined by full-matrix least-squares techniques based on F^2 for compounds **1**, **2**, **5**, and **6** and on F for compound **3**, respectively. Non-H atoms were refined with anisotropic displacement parameters. Structures were solved using SHELXS-2014 (for compounds **1**, **2**, **5**, and **6**) or SIR92 (for compound **3**) and refined using SHELXL-2014 (**1**, **2**, **4**, **5**, and **6**) or CRYSTALS (**3**) crystallographic software packages. Hydrogen atoms were refined with riding constraints. Drawings of molecules were performed using Diamond 3 software. X-ray crystallographic data in CIF format for 1, 2, 3, 5, and 6 are available as Supporting Information and also have been deposited with the CCDC with the following reference numbers: 1490383 (**1**), 1490384 (**2**), 1490382 (**3**), 1490386 (**5**), and 1490385 (**6**). For compound **4**, which is isostructural with compounds **1**, **2**, **3**, and **5**, we measured only the unit cell parameters. A summary of the crystallographic data and the structure refinement parameters is given in Table 1.

Magnetic Measurements. Magnetic data were obtained with a Quantum Design MPMS-5 SQUID susceptometer. All samples consisted of crushed crystals dispersed in grease to avoid orientation in field. Magnetic susceptibility measurements were performed in the 2−300 K temperature range.

Computational Details. *Ab initio* calculations were carried out with Molcas 7.6 program package for **1**, **3**, **4**, and **5** and Molcas 8.0 for **7**−**11** and were based on different structural models.[21] The calculated fragments of Ln, Ni, and W are shown in Figure S2. Due to the impossibility of including into one active space the magnetic orbitals from all magnetic centers, calculations were done for individual magnetic centers. In such calculations the other two metal ions were substituted by diamagnetic closed-shell ions. In the case of Ln^{III} fragment calculations, Ni^{II} was replaced with Zn^{II} and W^{V} was replaced with Ta^{V}, whereas in the case of Ni^{II} fragment calculations, Ln^{III} was substituted by Y^{III}-AIMP (*ab initio* embedding potential)[22] and W^{V} by La^{III}-AIMP respectively. Finally, in the case of the W^{V} fragment calculations, Ni^{II} was replaced with a Zn^{II}-AIMP. The Cholesky decomposition of the electron repulsion matrix was used with a threshold of 10^{-6} au to save disk space. The complete active space self-consistent field (CASSCF) calculations have been done within two basis set approximations, see Table S1 for details. The active space for lanthanides was set to seven 4f-type orbitals, for tungsten to five 5d-type orbitals, and for nickel to 10 orbitals (3d- and 4d-type) in order to take into account the double-shell effect.[23] The CASPT2 calculations have been carried out for nickel fragments. The imaginary shift for the zero order Hamiltonian was set to 0.05 eV. The IPEA shift was kept as default value, which is 0.25 Ha. The CASSCF/CASPT2 calculations were followed by the restricted active space state interaction (RASSI) method in order to include the spin−orbit interaction. The SINGLE_ANISO module[24] was used for the calculation of local magnetic properties of the mononuclear fragments. The exchange interactions between magnetic centers were simulated within the Lines model[25] by means of POLY_ANISO software[26] using the effective exchange Hamiltonian:

$$\hat{H}_{exch} = -J_{Ni-Ln}\hat{S}_{Ni}\cdot\hat{S}_{Ln} - J_{Ni-W}\hat{S}_{Ni}\cdot\hat{S}_{W} \quad (1)$$

This effective exchange Hamiltonian is diagonalized on the basis of the products of the *ab initio* calculated spin−orbit eigenstates of the metal fragments. On the basis of the exchange eigenstates, the magnetic moments are computed, and they are further used for the calculation of magnetic properties, such as magnetic susceptibility and molar magnetization. The only fitting parameters of the employed computational scheme are the exchange coupling parameters J and the intermolecular interaction, which is included in a mean-field approximation and is described by a single parameter zJ'. Their values are extracted from the fitting of magnetic susceptibility and magnetization data.

The B3LYP density functional has been used for DFT calculations within the ORCA 2.9.0 software.[27] Scalar relativistic effects were accounted for by second-order Douglas−Kroll−Hess Hamiltonian. The SVP Ahlrichs basis set was employed for all atoms.

RESULTS AND DISCUSSION

Synthesis and Crystal Structures. Compounds **1**−**6** have been obtained following the same procedure: the slow interdiffusion of an aqueous solution containing $Cs_3[W^{V}(CN)_8]$ and another one containing the corresponding $[Ni^{II}(valpn)Ln^{III}]$ heterodinuclear complex dissolved in acetonitrile. The crystallographic investigation showed that the six compounds have similar structures and possess the same angular trinuclear W−Ni−Ln core as the trimetallic complexes reported earlier.[16a]

The octacyanido−tungstate anion coordinates through one cyanido group into one of the apical positions of the nickel(II) ion. The main difference between these complexes and those previously reported arises from the nature of coordinated and/

DOI: 10.1021/acs.inorgchem.6b01669
Inorg. Chem. 2016, 55, 12158−12171

Table 1. Crystallographic Data and Refinement Parameters for Complexes 1−6

	1	2	3
chem formula	$C_{27}H_{32}N_{10}O_{10}NiYW$	$C_{27}H_{32}N_{10}O_{10}NiEuW$	$C_{27}H_{32}N_{10}O_{10}NiGdW$
M (g mol^{-1})	988.09	1051.14	1056.42
temp (K)	293	293	180
wavelength (Å)	0.71073	0.71073	0.71073
cryst syst	monoclinic	monoclinic	monoclinic
space group	$P2_1/c$	$P2_1/c$	$P2_1/c$
a (Å)	8.9506(5)	8.9747(3)	8.9103(3)
b (Å)	13.9237(6)	13.9587(4)	13.9215(5)
c (Å)	27.4023(15)	27.4653(9)	27.2730(10)
α(deg)	90.000	90.000	90.000
β (deg)	93.252(4)	93.266(3)	93.553(4)
γ (deg)	90.000	90.000	90.000
V (Å^3)	3409.5(3)	3435.13(19)	3376.6(2)
Z	4	4	4
D_c	1.925	2.032	2.078
μ (mm^{-1})	5.669	5.755	5.961
F(000)	1940	2036	1992
refinement on	F^2	F^2	F
goodness-of-fit	1.064	1.057	0.998
final R1, wR2 [$I > n\sigma(I)$]	0.0597, 0.1264 (n = 2)	0.0369, 0.0760 (n = 2)	0.0449, 0.0545 (n = 1.7)
R1, wR2 (all data)	0.0840, 0.1399	0.0467, 0.0792	0.0936, 0.1360
	4	5	6
chemical formula	$C_{27}H_{32}N_{10}O_{10}NiTbW$	$C_{27}H_{32}N_{10}O_{10}NiDyW$	$C_{27}H_{32}N_{10}O_{10}NiLuW$
M (g mol^{-1})	1058.10	1061.68	1074.15
temp (K)	293	293	293
wavelength (Å)	0.71073	0.71073	0.71073
cryst syst	monoclinic	monoclinic	orthorhombic
space group	$P2_1/c$	$P2_1/c$	$P2_12_12_1$
a (Å)	8.9603(65)	8.9520(2)	8.9298(4)
b (Å)	13.9385(74)	13.9264(3)	13.9422(7)
c (Å)	27.435(24)	27.3934(6)	30.8112(19)
α (deg)	90.000	90.000	90.000
β (deg)	93.050(66)	93.261(2)	90.000
γ (deg)	90.000	90.000	90.000
V (Å^3)	3421.6(43)	3409.58(13)	3836.0(4)
Z		4	4
D_c		2.068	1.860
μ (mm^{-1})		6.150	6.092
F(000)		2048	2068
refinement on		F^2	F^2
goodness-of-fit		1.191	1.055
final R1, wR2 [$I > n\sigma(I)$]		0.0413, 0.1033 (n = 2)	0.0840, 0.2182 (n = 2)
R1, wR2 (all data)		0.0454, 0.1065	0.0984, 0.2316

or crystallization solvent molecules. In compounds **1−6**, although crystals were grown from water/acetonitrile solutions, only coordinated and uncoordinated water molecules are found in the crystal structures. Let us discuss here only the crystal structure of the dysprosium derivative (Figure 1).

The dysprosium ion is placed in the outer, open compartment, being surrounded by eight oxygen atoms: two phenoxido and two methoxy oxygen atoms arising from the Schiff base [Dy1−O1 = 2.444(4); Dy1−O2 = 2.274(4); Dy1−O3 = 2.282(4); Dy1−O4 = 2.425(4) Å] and four oxygen atoms coming from the aqua ligands [Dy1−O5 = 2.420(5); Dy1−O6 = 2.414(5); Dy1−O7 = 2.400(5); Dy1−O8 = 2.357(4) Å]. We recall that, in the series of trinuclear [$Ni^{II}Ln^{III}W^{V}$] previously reported,[16a] the coordination sphere of the Ln^{III} ions is filled by oxygen atoms arising from the organic ligand and by four dmf molecules or three dmf ligands and one aqua ligand.

The nickel ion is located into the N_2O_2 compartment of the ligand and shows an elongated octahedral stereochemistry, with a N_2O_2 tetragonal base formed by the donor atoms of the organic ligand [Ni1−N1 = 2.027(5); Ni1−N2 = 2.005(5); Ni1−O2 = 2.033(4); Ni1−O3 = 2.011(4) Å], the apical position being occupied by an aqua ligand [Ni1−O9 = 2.242(4) Å], and a nitrogen atom arising from the cyanido bridge [Ni1−N3 = 2.106(5) Å]. Intramolecular Ni···Dy, Ni···W, and W···Dy distances are 3.477, 5.342, and 6.971 Å, respectively. The W−CN−Ni moiety is angular, with C−N−Ni = 162.7(5)°. The coordination polyhedron of the tungsten ion can be described using the so-called continuous shape measures analysis (CShM),[28] which indicates a distorted dodecahedral (DD) geometry, with one type A cyanido group as a bridging ligand.[17] The coordinated and uncoordinated water molecules are involved in an extended network of hydrogen bonds.

DOI: 10.1021/acs.inorgchem.6b01669
Inorg. Chem. 2016, 55, 12158−12171

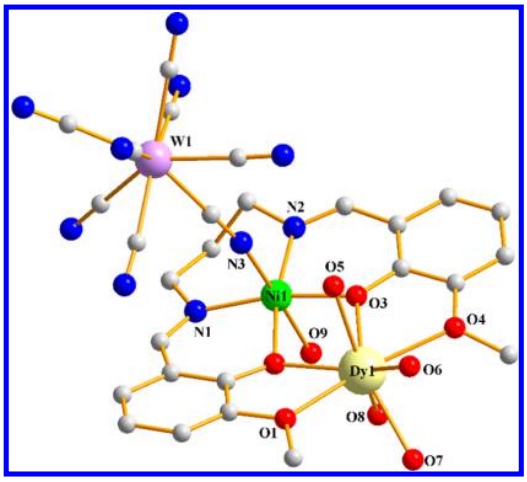

Figure 1. Perspective view of the trinuclear complex $[(CN)_7W(CN)\text{-}Ni(H_2O)(valpn)Dy(H_2O)_4]\cdot H_2O$, **5**.

At the supramolecular level, each trinuclear unit interacts through hydrogen bonds with 8 neighboring trinuclear units ($O5\cdots N4^{1}$ = 3.001, $O6\cdots N9^{2}$ = 2.741, $O8\cdots N7^{4}$ = 2.771, $O9\cdots N10^{5}$ = 2.841, $O9\cdots N5^{6}$ = 2.965, $N4\cdots O5^{1}$ = 3.006, $N5\cdots O9^{7}$ = 2.965, $N7\cdots O8^{9}$ = 2.771, $N9\cdots O6^{2}$ = 2.741, $N10\cdots O9^{10}$ = 2.841 Å) and two crystallization water molecules ($O7\cdots O_w10^{i}$ = 2.769, $N6\cdots O_w10^{ii}$ = 2.883 Å), which are further hydrogen-bonded to another two trinuclear units ($O10^{i}\cdots N6^{3}$ = 2.879, $O_w10^{ii}\cdots O7^{8}$ = 2.769 Å) [superscripts 1 = $-x$, $1-y$, $-z$; 2 = $1-x$, $1-y$, $-z$; 3 = $1+x$, $-1+y$, z; 4 = x, $-1+y$, z; 5 = $1-x$, $-0.5+y$, $0.5-z$; 6 = $-x$, $-0.5+y$, $0.5-z$; 7 = $-x$, $0.5+y$, $0.5-z$; 8 = $-1+x$, $1+y$, z; 9 = x, $1+y$, z; 10 = $1-x$, $0.5+y$, $0.5-z$; i = x, $-1+y$, z; ii = $-1+x$, y, z]. The result of these interactions is a complex 3-D supramolecular structure, a part of which is depicted in Figure 2. Selected bond distances for compound **5** are collected in Table 2.

Magnetic Properties. Magnetic behaviors of the yttrium, gadolinium, terbium, and dysprosium derivatives (**1**, **3**, **4**, and **5**, respectively) have been investigated in the 2–300 K temperature range. The $\chi_M T$ vs T and M vs H curves for these compounds are displayed in Figures 3 and 4.

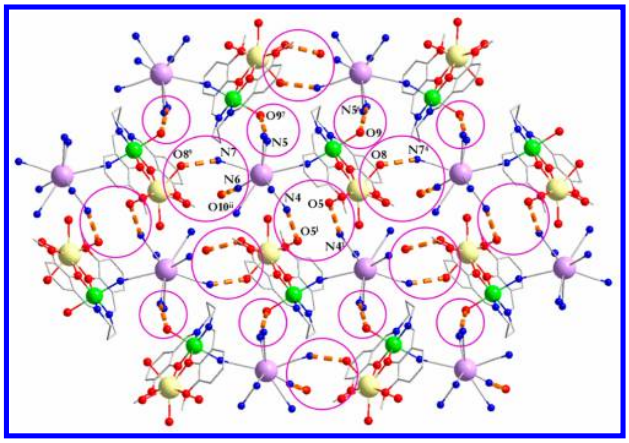

Figure 2. Detail of the packing diagram for compound **5** [superscripts 1 = $-x$, $1-y$, $-z$; 4 = x, $-1+y$, z; 6 = $-x$, $-0.5+y$, $0.5-z$; 7 = $-x$, $0.5+y$, $0.5-z$; 9 = x, $1+y$, z; ii = $-1+x$, y, z].

Table 2. Selected Bond Distances for Complexes 1–3, 5, and 6

	Complex **1**		
Ni1–N1	2.023(7)	Y1–O1	2.426(6)
Ni1–N2	2.018(7)	Y1–O2	2.263(6)
Ni1–N3	2.106(8)	Y1–O3	2.269(5)
Ni1–O2	2.043(6)	Y1–O4	2.421(6)
Ni1–O3	2.014(6)	Y1–O5	2.419(7)
Ni1–O9	2.238(6)	Y1–O6	2.412(6)
		Y1–O7	2.398(7)
		Y1–O8	2.357(6)
	Complex **2**		
Ni1–N1	2.036(5)	Eu1–O1	2.470(4)
Ni1–N2	2.011(5)	Eu1–O2	2.306(3)
Ni1–N3	2.100(5)	Eu1–O3	2.317(3)
Ni1–O2	2.039(4)	Eu1–O4	2.460(4)
Ni1–O3	2.017(4)	Eu1–O5	2.476(4)
Ni1–O9	2.244(4)	Eu1–O6	2.459(4)
		Eu1–O7	2.459(4)
		Eu1–O8	2.410(4)
	Complex **3**		
Ni1–N1	2.10(1)	Gd1–O1	2.44(1)
Ni1–N9	2.01(1)	Gd1–O2	2.306(9)
Ni1–N10	2.01(1)	Gd1–O3	2.304(8)
Ni1–O2	2.007(8)	Gd1–O4	2.44(1)
Ni1–O3	2.033(9)	Gd1–O5	2.44(1)
Ni1–O9	2.216(9)	Gd1–O6	2.442(8)
		Gd1–O7	2.45(1)
		Gd1–O8	2.385(9)
	Complex **5**		
Ni1–N1	2.027(5)	Dy1–O1	2.444(4)
Ni1–N2	2.005(5)	Dy1–O2	2.274(4)
Ni1–N3	2.106(5)	Dy1–O3	2.282(4)
Ni1–O2	2.033(4)	Dy1–O4	2.425(4)
Ni1–O3	2.011(4)	Dy1–O5	2.420(5)
Ni1–O9	2.242(4)	Dy1–O6	2.414(4)
		Dy1–O7	2.400(5)
		Dy1–O8	2.357(4)
	Complex **6**		
Ni1–N1	2.00(2)	Lu1–O1	2.42(2)
Ni1–N2	2.01(2)	Lu1–O2	2.201(18)
Ni1–N3	2.13(3)	Lu1–O3	2.236(16)
Ni1–O2	2.03(2)	Lu1–O4	2.44(2)
Ni1–O3	2.019(17)	Lu1–O5	2.32(2)
Ni1–O9	2.32(2)	Lu1–O6	2.397(19)
		Lu1–O7	2.25(2)
		Lu1–O8	2.30(2)

Let us start with **1**, the yttrium derivative, which gives directly information about the Ni^{II}–W^{V} exchange interaction. The value of the $\chi_M T$ product at room temperature is 1.70 $cm^3\ mol^{-1}\ K$, which is in good agreement with what is to be expected for two noninteracting paramagnetic centers, one with $S = 1$ (Ni^{II}) and the second carrying one unpaired electron, W^{V} ($S = 1/2$). The value of the $\chi_M T$ product increases on lowering the temperature, reaching a maximum around 20 K, which indicates a ferromagnetic interaction ($S = 3/2$ ground state). Below 20 K, the $\chi_M T$ product decreases down to 1.0 $cm^3\ mol^{-1}\ K$ at 2 K.

In the case of the gadolinium derivative, **3**, the room temperature value of the $\chi_M T$ product (9.20 $cm^3\ mol^{-1}\ K$) corresponds to the three magnetically isolated metal ions (Ni^{II}, Gd^{III}, and W^{V}). Upon cooling, $\chi_M T$ increases slowly, then more

DOI: 10.1021/acs.inorgchem.6b01669
Inorg. Chem. 2016, 55, 12158–12171

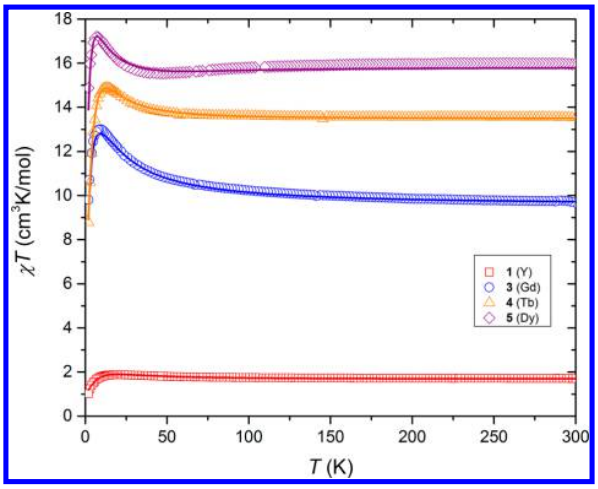

Figure 3. Experimental (symbols) and calculated (lines) powder magnetic susceptibility for **1** and **3**−**5**.

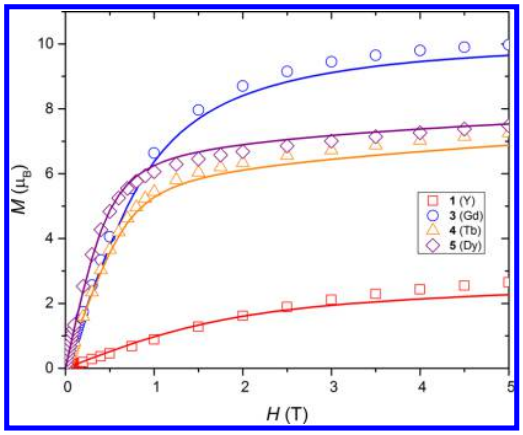

Figure 4. Experimental (symbols) and calculated (lines) powder magnetization for **1** and **3**−**5** at T = 2 K.

and more, reaching a maximum value of 13.1 cm^3 mol^{-1} K at 10 K, corresponding to the S = 5 ground state. Below this temperature, the value of the $\chi_M T$ product decreases down to ~9.7 cm^3 mol^{-1} K at 2 K.

Ionic Magnetic Anisotropy in 1, 3, 4, and 5. *Ab Initio Calculations for W Centers.* The fragment *ab initio* calculations on tungsten ions show that the ground state is well separated from the excited states by about 33000 cm^{-1} in all investigated compounds (see Table S2). This is indeed to be expected since the ligand field created by the cyanide groups is generally very strong. In the present case the ligand field is further enhanced by the diffuse character of the 5d orbitals of tungsten. Although the spin−orbit coupling in W^V is strong, the large energy separation minimizes the admixture of the excited states via spin−orbit interaction (Table S3), resulting in almost isotropic spin S = 1/2 of W^V (Table S4). Considering this very large splitting CASPT2 calculations were not performed on tungsten fragments.

Ab Initio Calculations for Ni Centers. The ground state of nickel in the investigated compounds is an orbitally non-degenerate spin triplet $^3A_2$ state. In the case of a free ion, the ground state of Ni^{II} is a ^3F multiplet, while the first excited multiplet is ^3P. In the presence of an octahedral ligand field, the ground orbital multiplet ^3F splits into the ground triplet $^3A_2$ and two excited triplets $^3T_1$ and $^3T_2$. In the case of an axial distortion of the octahedral ligand field, each triplet $^3T_1$ and $^3T_2$ splits further into ^3A and ^3E. From Table S5 we observe that the ground $^3A_2$ state is well stabilized, the first excited triplet being placed at about 8000 cm^{-1} higher in energy. On the other hand, the spin−orbit coupling is relatively small, ca. 650 cm^{-1},[29] which means that the admixture of the excited states via spin−orbit coupling is relatively small too and as a consequence a small zero-field splitting (ZFS) is expected. This is observed indeed as well as the weak anisotropy of g-factors (Table 3) which are all close to 2.

Table 3. Low-Lying CASPT2/RASSI Spin−Orbit Energies (cm^{-1}) and the g-Factors of the Ground Spin Triplet State of the Ni Fragments

1	3	4	5
Spin−Orbit Energies (cm^{-1})			
0	0	0	0
12	12	12	12
16	15	16	16
7518	7719	7533	7588
7642	7839	7648	7707
7889	8071	7884	7940
g-Factors in the Ground Triplet States			
2.30	2.28	2.29	2.29
2.27	2.25	2.26	2.27
2.18	2.17	2.18	2.17

Ab Initio Calculations for Ln Centers. After the calculation of spin-free term energies by the CASSCF approach (Table S6), the spin−orbit multiplets for the Gd^{III}, Tb^{III}, and Dy^{III} fragments were calculated by the SO-RASSI program. The resulting spin−orbit energies are shown in Table 4.

Table 4. Low-Lying CASSCF/RASSI Spin−Orbit Energies (cm^{-1}) and the g-Factors of the Ground Multiplets of the Ln^{III} Fragments

3 (Gd)[a]	4 (Tb)	5 (Dy)[a]
Spin−Orbit Energies (cm^{-1})		
0	0.00	0
0.40	1.09	119
0.65	75	174
0.88	84	214
	161	239
	194	272
	230	383
	262	532
	272	
	386	
	389	
	459	
	460	
g-Factors in the Ground Multiplet[b]		
1.99	0.0	0.02
1.99	0.0	0.03
1.99	17.5	19.8

[a] 2-fold degenerate energy levels corresponding to Kramers doublets.[30] [b] The g-factor is given for S = 7/2 of Gd and for $\tilde{s}$ = 1/2 of Tb and Dy fragments, respectively.

DOI: 10.1021/acs.inorgchem.6b01669
Inorg. Chem. 2016, 55, 12158−12171

The ground state of gadolinium is the octet ^8S, in which each orbital of the 4f shell is occupied by a single electron. The lowest excited state corresponds to the reversal of the spin of one electron to a total spin sextet. Such configurations are much higher in energy because of the large Hund's rule intersection for seven unpaired electrons. Indeed, the first excited spin sextet lies at about 41000 cm^{-1} (Table S6). Given this large excitation energy, a very small effect of the spin−orbit coupling in the ground state is expected. Due to limited disk space only a part of excited states could be admixed within the SO-RASSI program: all 48 spin sextet states, 120 (out of 392) spin quartet states, and 113 (out of 784) spin doublet states. The resulting ZFS of the ground $S = 7/2$ on Gd^{III} is smaller than one wavenumber, while $g_x \approx g_y \approx g_z$ (Table 4), which shows that Gd^{III} is almost isotropic.

The ground ionic multiplet of Tb^{III} free ion is $^7F_6$. In the spin−orbit mixing calculations by SO-RASSI we included all 7 septet states, all 140 quintet states, 113 (out of 588) triplet states, and 123 (out of 490) singlet states. The computed spin−orbit energies of the Tb^{III} center are shown in Table 4. Despite a small splitting, the group of 13 multiplets arising from the atomic $^7F_6$ is well separated from the group of 11 multiplets arising from the crystal-field splitting of the atomic $^7F_5$ multiplet (Table S7). The Tb^{III} ion is a non-Kramers ion, therefore its transversal g-factors, g_x and g_y, in the ground doublet are exactly zero, in virtue of Griffith's theorem.[31]

The low-lying multiplet spectrum of Dy^{III} center consists of eight Kramers doublets (KDs) originating from the crystal-field splitting of the ground atomic multiplet $^6H_{15/2}$ (Table 4). Again, as in the case of the Tb^{III} fragment, the manifold of these crystal-field states is well separated from a group of seven KDs originating from the first excited atomic multiplet $^6H_{13/2}$ (Table S7).

Exchange Interaction and Magnetization Blocking in 1, 3, 4, and 5. *Simulation of Magnetism.* The exchange interaction between magnetic centers was simulated within the Lines model by using the POLY_ANISO program. The results obtained from the larger basis set fragment calculations were used for the computation of magnetic properties for all investigated compounds. Three low-lying spin−orbital states from Ni^{II}, two states from W^V, 8 states from Gd^{III}, 13 states from Tb^{III}, and 16 states from Dy^{III} were included in the exact diagonalization of the exchange matrix, which resulted in 6 exchange states for **1**, 48 states for **3**, 78 states for **4**, and 96 states for **5**.

To estimate the exchange coupling constant between Ni^{II} and W^V centers in **1**, BS-DFT calculations were performed and Yamaguchi's formula was used.[32] The calculated value is 9.9 cm^{-1}, which shows that the exchange interaction between Ni^{II} and W^V is ferromagnetic and relatively strong. The exchange interaction between Ni^{II} and W^V centers in compounds **3**, **4**, and **5** is expected to be of the same order of magnitude and the same sign, since these compounds have isostructural cores.

The best fit of magnetic susceptibility data is given by the parameters shown in Table 5, and the low-lying exchange spectra are shown in Table 6. As we can see from Figure 3, the calculated magnetic susceptibility is in good agreement with the experimental data. In addition, the DFT calculated value for Ni^{II}−W^V exchange interaction is in good agreement with the fitted values. By using the extracted exchange coupling constants from the magnetic susceptibility fitting procedure, the magnetization curves have been calculated and are shown in Figure 4. The good agreement of calculated and experimental data confirms the accuracy of the employed theoretical calculations.

Since tungsten is isotropic, nickel is weakly anisotropic, and the lanthanide ion (terbium or dysprosium) is very anisotropic, it is expected that in the ground exchange doublet state the magnetic moments of the former ions will be aligned along the main magnetic axis of the lanthanide site. Indeed, according to the calculations the magnetic moments of tungsten and nickel look along the same direction as the magnetic moment of the lanthanides (Figure 5).

Table 5. Fitted Exchange Coupling Constants in Eq 1 (cm^{-1})

pair/compound	1	3	4	5
J(Ln−Ni)		3.46	3.0	2.5
J(Ni−W)	16.08	21.6	22.0	24.0
zJ'	−0.098	−0.07	−0.05	−0.05

Table 6. Low-Lying Exchange Spectra (cm^{-1}) for 1−5 and the g-Factors for Their Ground Exchange Doublet

1[a]	3	4[a]	5
Low-Lying Exchange Spectral Data (cm^{-1})			
0	0	0	0
12.5	0.004	8.27	1.8×10^{-3}
33.2	1.27	18.9	6.74
	1.39	20.3	6.74
	2.04	42.6	15.90
	2.76	51.6	15.92
	2.91	79.4	16.67
	4.73	87.9	16.69
	4.74	95.6	44.31
	9.37		44.32
	9.37		
Main Values of the g-Factors in the Ground Exchange Doublet			
1.89	0	0.19	0
3.43	0	0.28	0
4.31	19.84	23.46	25.70

[a]2-fold degenerate energy levels corresponding to exchange Kramers doublets.

The Origin of Strong Ferromagnetic Coupling in Ni−W Pairs. A common feature shared by the investigated compounds is the strong ferromagnetic exchange interaction between Ni and W ions, found by both DFT and the fitting procedure. Given its crucial importance for the discussed SMM properties (see below), we analyze this exchange interaction in detail. First glance at the structure of these compounds does not testify that the magnetic orbitals are orthogonal to each other, thus fulfilling the necessary condition for ferromagnetic exchange interaction. We show here that the origin of ferromagnetism in the Ni−W pairs of our compounds is due to a strong suppression of antiferromagnetic kinetic contribution via a mechanism specific to d^1 octacyanometalates.[33] This mechanism was first proposed for the rationalization of exchange interaction in polynuclear complexes and magnetic networks containing $Mo(CN)_8^{3-}$, $W(CN)_8^{3-}$, and $Nb(CN)_8^{4-}$ octacyano-bridged with Mn^{II} ions,[33] and later was found operative in other series of compounds.[17]

Analyzing the magnetic orbitals of Ni(II) and W(V) ions obtained in DFT calculations (Figure 6), we observe that the

DOI: 10.1021/acs.inorgchem.6b01669
Inorg. Chem. 2016, 55, 12158−12171

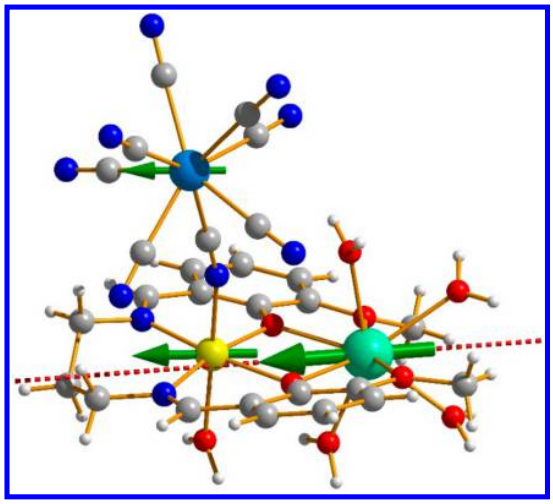

Figure 5. Main magnetic axis (dashed line) and local magnetic moments (arrows) in the ground exchange doublet of **5**.

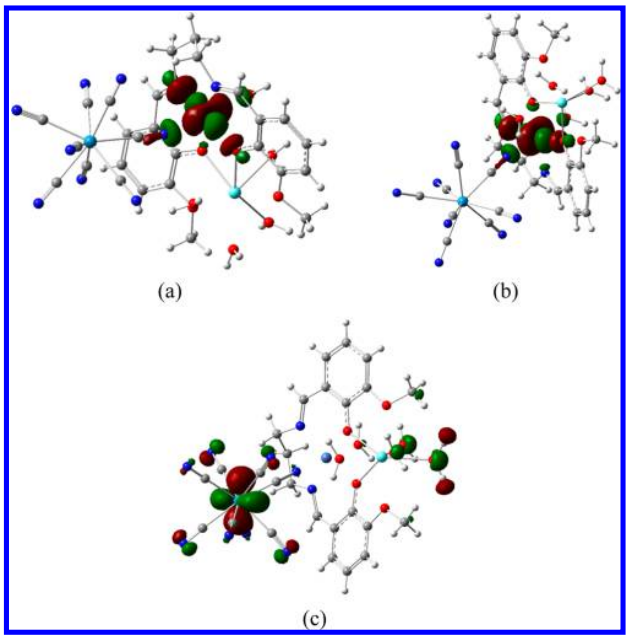

Figure 6. Localized magnetic orbitals of Ni (a, b) and W (c).

W−C bond is directed along the nodal plane of the W magnetic orbital. Figure 6 shows that the tail of Ni orbitals on the bridging cyanide group is mainly of σ type, whereas the W orbital has only π contributions from CN^- on it. Therefore, due to symmetry reasons, the overlap of σ (Ni) and π (W) is almost zero.

Considering that the electron transfer integral is proportional to this overlap, we conclude that the antiferro contribution is suppressed. On the other hand, the d_σ orbital of W is empty and the ferromagnetic interaction is favored by the electron transfer from the Ni site to the empty d orbitals of W (Figure 7). This is the well-known Goodenough ferromagnetic mechanism.[34] Therefore, the observed strong ferromagnetism for the Ni−W metal pair is due to the Goodenough mechanism in combination with the direct exchange, which is always present and ferromagnetic. A similar situation was found for Mo^V, Nb^{IV}, and W^V octacyano-bridged with Mn^{II} ions in the

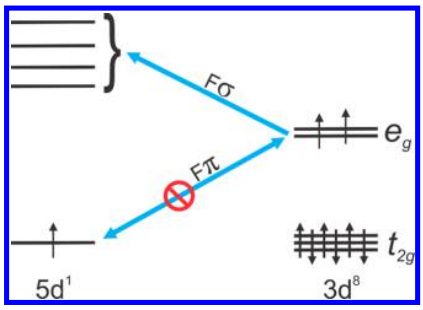

Figure 7. Scheme of the ferromagnetic kinetic contribution to the exchange interaction in the W^V−Ni^{II} pair.

earlier investigated series of compounds.[33] In that series the antiferromagnetic kinetic part also played a role via the electron transfer from the molybdenum magnetic orbital to the manganese magnetic orbitals, which could occur through the π orbitals of the cyanide bridge. On the contrary, in the present case, the t_{2g} orbital levels of Ni^{II} are double occupied (Figure 7) and such a transfer is not relevant for the exchange interaction. Another example of ferromagnetic interaction between metal pairs bridged by cyanide groups was reported in some $\{Cu^{II}$−$[W^V(CN)_8]\}$ systems.[35] The reason for the observed ferromagnetism is similar to the one discussed here: the magnetic electrons of the W ions delocalize in the cyanide orbitals of π type, while the magnetic electrons of copper ions (Ni in our case) delocalize in the cyanide orbitals of σ type, thus, favoring the ferromagnetic interaction.

Magnetization Blocking. In order to put to test the presence of slow relaxation of magnetization, ac measurements were carried out on **1**−**5** in the temperature range 2−15 K at different frequencies (Figure S1). None of the studied compounds showed any maxima in the out-of-phase χ'' component, despite the strong anisotropy of Tb^{III} and Dy^{III} ions. To understand the lack of SMM behavior we further analyzed the results obtained from *ab initio* calculations. Complexes **1** and **4** have an odd number of electrons, which gives rise to an exchange spectrum composed from Kramers doublets (Table 6).[30] As it was shown before, strong axiality of the ground doublet of a compound is the necessary condition for the manifestation of magnetization blocking.[8] The axiality of a KD is measured by the smallness of transversal *g*-factors, g_x and g_y, of the exchange doublet. As we can see from Table 6, the transversal *g*-factors in the ground exchange doublet of **1** and **4** are relatively large. Given the fact that the tunneling splitting Δ_{tun} arising from the Zeeman interaction of transversal magnetic moments with the external magnetic field (which is always present in a crystal) is proportional to g_x and g_y, a large Δ_{tun} is expected. As a result, the tunneling relaxation of magnetization will be very fast, which explains well the lack of SMM behavior in these compounds. In **3** and **5** we deal with the Ising exchange doublets because of an even number of electrons in these complexes. The transversal components of an Ising doublet are exactly zero. The transversal *g*-factors, g_x and g_y, are zero according to Griffith's theorem (Table 6), while Δ_{tun} in these compounds has an intrinsic origin. As we see from Table 6, its values are relatively large, $\sim 10^{-3}$ cm^{-1} (the energy gap of the ground doublet), which explains well why neither of these complexes exhibits slow relaxation of magnetization.

***Ab Initio* Investigation of 7−11.** Complexes **7**−**11** were previously reported in ref 16a. These compounds are relevant for the present study because their core is similar to that in **1**−**5**

DOI: 10.1021/acs.inorgchem.6b01669
Inorg. Chem. 2016, 55, 12158−12171

and, moreover, one of the compounds is an SMM. Applying the same theoretical approach as for **1**−**5**, we investigate their magnetic properties and try to understand why only $[(CN)_7W(CN)Ni(H_2O)(valdmpn)Tb(dmf)_{2.5}(H_2O)_{1.5}]\cdot H_2O\cdot 0.5dmf$ **8b** (Figure 8) is an SMM.

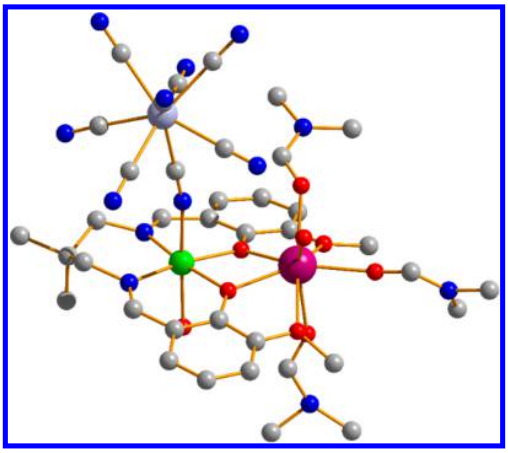

Figure 8. Structure of **8b**. Hydrogen atoms are omitted for clarity.

Ionic Anisotropy in 7−**11.** The calculated spin−orbit energies of the lanthanide fragments are shown in Table S10. We can see that the ZFS on the Gd^{III} center is very small and as a result its ground octet is obtained practically isotropic, $g_x \approx g_y \approx g_z$. We note that the ZFS of the Gd^{III} ion in **7** is about twice smaller than in **3**.

By analyzing the low-lying multiplets of Tb^{III} ions one notices an important feature: the tunneling splitting of the ground Ising doublet in **8b** is obtained almost ten times smaller than in **8a**, which tells us that Tb is much more axial in the former complex. This difference in axiality plays a key role for understanding the different blocking properties of these two complexes experimentally observed. To compare, the tunneling splitting of the Tb^{III} ground doublet in **4** is ca. 1.1 cm^{-1}, even larger than in **8a**.

Both Dy^{III} and Er^{III} centers have relatively large components of the transversal components of the *g*-tensor in their ground doublet (Table S10), which diminishes the chances of the respective complexes of being SMM. In the case of the Ho^{III} ion, the tunneling splitting of the ground doublet is about 6 cm^{-1}, i.e., very large. This large tunneling gap of the Ho^{III} ion excludes the SMM behavior in **10**.

The calculated spin−orbit energies of Ni^{II} and W^{V} fragments are shown in Tables S8 and S9. We notice a small ZFS on all Ni^{II} fragments, similar to the calculated ZFS of compounds **1**−**5**. As a result, the ground triplet is obtained slightly anisotropic. The tungsten fragments show almost isotropic ground state, for the same reason as in **1**−**5** compounds, due to a strong crystal field induced by cyanide groups.

Exchange Interaction. The exchange interaction was treated within the Lines model as before, employing the Hamiltonian from eq 1. For Ni^{II}, W^{V}, Gd^{III}, Tb^{III}, and Dy^{III} ions, the same number of states were included in the exact diagonalization of the exchange Hamiltonian as for **1**−**5**. For Ho^{III} and Er^{III}, 17 and 16 states, respectively, were taken into account. The exchange coupling constants corresponding to the best fitting of magnetic susceptibility data (Figure 9) are given in Table 7, while the obtained low-lying exchange spectra are shown in Table 8.

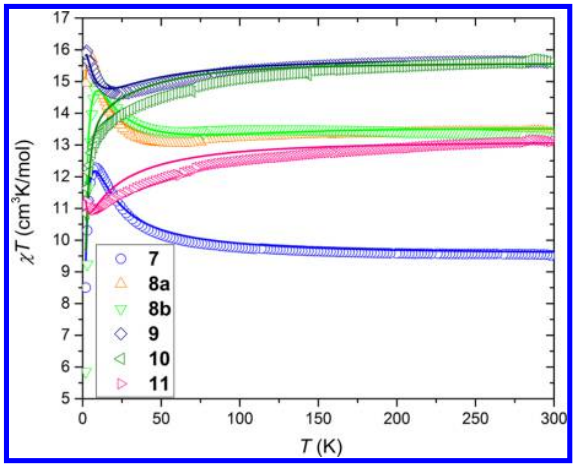

Figure 9. Experimental (symbols) and calculated (lines) powder magnetic susceptibility for **7**−**11**. Experimental curves for **7**, **8a**, and **11** were upscaled by 2% and for **9** by 1%.

Table 7. Fitted Lines Exchange Coupling Constants (cm^{-1})

pair/ compound	7	8a	8b	9	10	11
J(Ln−Ni)	2.4	2.5	3.5	1.1	1.5	1.0
J(Ni−W)	16.0	19.8	26.0	16.1	13.0	12.9
zJ′	−0.07	−0.011	−0.05	−0.013	0.05	0.015

Table 8. Energies of the Low-Lying Exchange Spectra (cm^{-1}) and the *g*-Factors for Their Ground Exchange Doublets of 7−**11**

7	8a[a]	8b[a]	9	10[a]	11
Energies of the Low-Lying Exchange Spectra (cm^{-1})					
0	0	0	0	0	0
0.009	6.42	7.41	0.009	6.35	0.064
0.66	9.31	12.0	2.87	9.75	1.12
0.80	18.4	23.7	2.90	15.6	1.25
1.14	34.9	44.2	10.2	19.5	7.94
1.74	44.6	58.2	10.2	26.3	7.95
1.81			11.9	28.3	9.51
3.21			11.9	32.6	9.54
3.22			30.8	36.0	24.8
7.09					
g-Factors in the Ground Exchange Doublet States					
0	0.026	0.002	0	1.82	0
0	0.033	0.003	0	3.49	0
19.60	23.2	23.5	23.9	11.2	19.4

[a]2-fold degenerate energy levels corresponding to Kramers doublets.

As we can see from Table 7, the exchange coupling parameters for Ln^{III}−Ni^{II} and Ni^{II}−W^{V} interactions are of the same order as for complexes **1**−**5**. This is the result of similar core structures in the two series of compounds.

Magnetization Blocking. In an attempt to explain why **8b** is SMM, while **8a** and **4** are not, we analyze the transversal *g*-factors of their ground doublet states (Table 8). Noticeably, the g_x and g_y values of **8b** are ten times smaller than the corresponding values of **8a**, and about 100 times smaller than these values in **4**, which means that the ground doublet in the

DOI: 10.1021/acs.inorgchem.6b01669
Inorg. Chem. 2016, 55, 12158−12171

former compound is the most axial among them. This explains well why only **8b** possesses slow relaxation of magnetization. The much lower axiality of the other compounds in the two series explains why none of them exhibits SMM behavior. The *ab initio* constructed barrier is shown in Figure 10.[36]

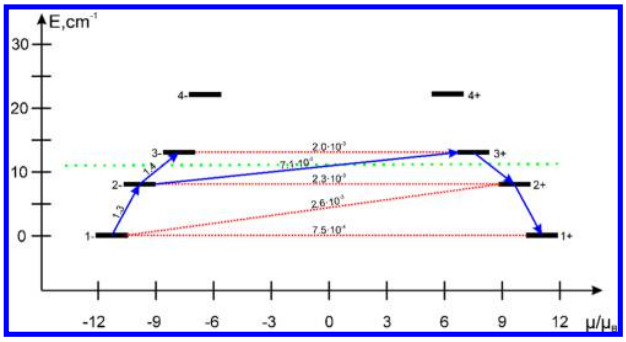

Figure 10. Low-lying exchange spectrum and the position of the magnetization blocking barrier (dashed green line) in **8b**. Each exchange state is placed in accordance with the value of its magnetic moment (bold black lines). The numbers show the average matrix elements connecting the corresponding states, and the relaxation path is outlined by blue arrows.

The relaxation path can be outlined by connecting the states with the largest transition magnetic moments (shown by blue arrows in Figure 10). The calculated blocking barrier matches well the experimentally extracted one (green dashed line, 10.8 cm^{-1}).

Prospects To Enhance the SMM Performance of Polynuclear Complexes. The geometry of the environment of Ln ions in the investigated complexes (Figure 1) does not provide a pronounced axial crystal field, resulting in relatively large transversal components of the *g*-tensor in the ground doublets of Kramers Ln ions and relatively large intrinsic tunneling gaps in the ground doublets of non-Kramers Ln ions (Tables 4 and S10). These are sufficiently large to preclude magnetization blocking on individual Ln ions (including Tb(III) in **8b**) if one disregards the interaction with Ni and W ions. It is well-known, however, that the polynuclear complex can exhibit strong SMM properties even when the entering metal ions are weekly anisotropic, the prominent example being the Mn_{12}(acac).[1] In the present case we have three magnetic metal ions, one (Ln) being strongly anisotropic: more surprising is the absence of magnetization blocking in the two investigated series of compounds except **8b**. The reason is the specific exchange and ZFS interaction in the Ni−W unit.

As the theoretical analysis shows, the exchange interaction between Ni(II) and W(V) ions is strongly ferromagnetic (Tables 5 and 7), leading to a strong stabilization of the spin S = 3/2 of the pair. This is further split by ZFS on Ni(II) ion, Table 3 (W(V) is practically isotropic), resulting in three KDs for the Ni−W unit (Table 9). The lowest two of them correspond to the splitting of S = 3/2 spin at this unit in two KDs. In the case of pure axial ZFS, described by the Hamiltonian DS_z^2, the two resulting KDs will be of $|\pm 1/2\rangle$ and $|\pm 3/2\rangle$, respectively, where the numbers are the projections M_S of S = 3/2 on the anisotropy axis (z). In the case of pure spin state, the first Kramers doublet will be characterized by the *g*-factors $g_x = g_y = 4$, $g_z = 2$, and the second one by $g_x = g_y = 0$, $g_z = 6$. Comparing these *g*-factors with the ones for the lowest two KDs of the Ni−W dimer (Table 9), we conclude that the ground one is close to $|\pm 1/2\rangle$ and the first excited one to $|\pm 3/2\rangle$. This is obviously the consequence of the positive axial ZFS on the Ni(II) site. The highest KD, corresponding to almost net S = 1/2 of the Ni−W unit, is isotropic (Table 9) as expected.

Table 9. Energies (cm^{-1}) and *g*-Factors for Low-Lying Exchange KDs in the Ni−W Group

E_1	g_i	E_2	g_i	E_3	g_i
0	4.7	7.9	0.5	43.5	2.2
	3.6		0.5		2.3
	2.0		6.2		2.3

The ground states of the NiLnW complexes mainly originate from the exchange interaction of the ground doublet of Ln(III) ion with the ground $|\pm 1/2\rangle$ doublet of the Ni(II)−W(V) dimer. The latter is rather an easy-plane doublet, meaning that its coupling to the ground doublet of Ln(III) ion will have larger transversal *g*-factors or intrinsic gaps than if the latter would be exchange coupled to just a conventional spin doublet. In other words, the coupling of a Ln(III) ion to the Ni(II)−W(V) dimer, as in the present case, is less efficient from the viewpoint of SMM performance than its coupling to an isotropic S = 1/2 (radical, a Cu(II) ion, etc.). That is, the coupling of Ln(III) to the Ni−W group will result in a weaker enhancement of SMM properties of the former than if it would be coupled to a simple S = 1/2. We can understand, therefore, why only **8b** is found to show a magnetization blocking: the relatively weak enhancement of blocking properties due to complexation to the Ni−W group was sufficient to turn into SMM only the most axial Ln ion in the two series, the Tb(III) in **8b** (Table 8).

To elucidate the factors which could enhance the SMM properties of the complexes, we investigated the modification of the axiality of low-lying exchange KDs in **8a** and **8b** under the variation of the ZFS tensor on the Ni site (Tables 10 and 11, respectively). First we checked whether the exclusion of rhombic components of ZFS will make important differences. Column 3 in the tables shows that the axiality of the ground exchange KD becomes only worse for pure axial ZFS with D > 0. The reason is that the rhombic terms of ZFS admix the excited $|\pm 3/2\rangle$ doublet of Ni−W to the ground $|\pm 1/2\rangle$ doublet, thus contributing to the enhancement of its axiality and of the ground doublet of the entire NiLnW system. The situation improves only a little when we chose the main anisotropy axis on Ni(II) parallel to the main magnetic axis on the Tb(III) ion (column 2 in the tables). The axiality enhances drastically (the transversal *g*-factors drop by 3 orders of magnitude) when we change the sign of D keeping the anisotropy axis on Ni and main magnetic axis on Tb parallel to each other (column 4 in the tables). Finally, we consider the case of an isotropic Ni(II) ion, resulting in an isotropic nonsplit ground term S = 3/2 of the Ni−W unit. We find that such a situation corresponds to the highest axiality of the ground state (column 1 in the tables), i.e., is the most favorable for SMM performance of our trinuclear complexes. As a matter of fact, in the absence of ZFS on Ni(II) all compounds in the two series investigated here (except those containing Y and Gd) would be SMMs.

Generalizing the results of the performed analysis we conclude that the coupling of weakly anisotropic magnetic units to strongly anisotropic ones (lanthanide ions) will result in a drastic enhancement of axiality of the low-lying exchange

DOI: 10.1021/acs.inorgchem.6b01669
Inorg. Chem. 2016, 55, 12158−12171

Table 10. Energies (cm^{-1}) and *g*-Factors for Lowest-Lying Exchange KDs in 8a

Ni-isotrop	D(Ni)‖Z(Tb)	D(Ni):Z arbitrary	$-D$(Ni)‖Z(Tb)	unmodified[a]
		Energies (cm^{-1})		
0	0	0	0	0
4.4	5.3	6.0	7.0	6.4
9.3	9.5	12.5	10.3	9.3
14.6	18.0	17.6	17.2	18.4
		g-Factors		
2.7×10^{-4}	0.033	0.029	0.0062	0.026
2.8×10^{-4}	0.048	0.041	0.0069	0.033
23.7	22.8	23.2	23.2	23.2
0.099	0.015	0.0084	0.085	0.058
0.10	0.071	0.065	0.095	0.068
19.8	18.7	18.6	20.1	18.8
0.096	0.0032	0.017	0.057	0.0031
0.10	0.070	0.068	0.099	0.086
15.8	18.1	17.2	15.39	18.36
5.4×10^{-4}	0.0069	0.020	0.022	0.0046
5.8×10^{-4}	0.0070	0.025	0.033	0.0080
11.8	12.8	13.4	13.1	12.5

[a]Calculation similar to Table 8.

states and, therefore, of the SMM performance of the complex only if the axial anisotropy of the formers is negative and directed parallel to the main magnetic axis of the former. While meeting these requirements will demand great engineering efforts from synthetic chemists, the main finding of our analysis is that coupling of strongly axial metal ions with pure isotropic ones will result in even stronger SMM properties. The emerging recommendation in the case of mixed lanthanide–transition metal complexes is the use of pure isotropic transition metal ions such as Mn(II), Fe(III), Cr(III), etc. A similar conclusion was drawn in the investigation of a series of anisotropic Co(II) complexes.[36]

CONCLUSIONS

In this work we presented the synthesis, crystal structures, magnetic behavior, and *ab initio* calculations for $[(CN)_7W(CN)Ni(H_2O)(valpn)Ln(H_2O)_4]\cdot H_2O$, where Ln = Y **1**, Eu **2**, Gd **3**, Tb **4**, Dy **5**, Lu **6**. Calculations show the existence of ferromagnetic interaction between the magnetic centers and that the comparison of calculated and experimental data for both $\chi_M T$ vs T and M vs H is remarkably good. Ac magnetic measurements revealed the absence of SMM behavior which was well explained by the relatively large transversal components of the **g**-tensor in the case of ground-state exchange Kramers doublets in **1** and **4** and by the large intrinsic tunneling gaps in the ground doublets of **3** and **5**. For the sake of comparison, we studied a series of similar compounds **7**–**11** by *ab initio* methods. This series does not show magnetization blocking too, except for one single compound **8b**. The calculations confirm that this only SMM complex, besides the similar core structures, has a significantly more axial ground state, compared to isometallic compounds **4** and **8a**. An important feature for the entire series is the strong ferromagnetic coupling between Ni(II) and W(V), which is found to be due to an almost perfect trigonal dodecahedron geometry of the octacyano wolframate fragment. The reason why only **8b** is an SMM is explained by positive zero-field splitting on the nickel site, precluding magnetization blocking in complexes with fewer axial Ln ions than in **8b**. Further analysis has shown that in the absence of ZFS on Ni(II) all compounds in the two series (except those containing Y and Gd) would be SMMs. The same situation arises for perfectly axial ZFS on Ni(II) with the main anisotropy axis parallel to the main magnetic axis of Ln(III) ions. In all other cases the ZFS on Ni(II) will worsen the SMM properties. The general conclusion is that the design of efficient SMMs on the basis of such complexes should involve isotropic or weekly anisotropic

Table 11. Energies (cm^{-1}) and *g*-Factors for Lowest-Lying Exchange KDs in 8b

Ni-isotrop	D(Ni)‖Z(Tb)	D(Ni):Z arbitrary	$-D$(Ni)‖Z(Tb)	unmodified
		Energies (cm^{-1})		
0	0	0	0	0
6.2	4.1	2.2	10.8	7.4
13.2	7.4	5.9	18.2	12.0
20.6	22.6	21.8	22.4	23.7
		g-Factors		
2.5×10^{-5}	0.0033	0.0046	6.0×10^{-5}	0.0020
2.5×10^{-5}	0.0041	0.0053	6.1×10^{-5}	0.0025
23.7	22.4	22.0	23.7	23.5
0.0074	0.0065	0.0056	0.0054	0.0056
0.0075	0.0092	0.0067	0.0056	0.0079
19.9	21.3	22.0	20.0	20.0
0.0069	0.010	0.010	0.0027	0.0037
0.0078	0.011	0.011	0.0038	0.0081
16.0	16.3	16.0	15.0	17.0
7.1×10^{-5}	5.5×10^{-5}	7.7×10^{-6}	0.0021	8.6×10^{-5}
7.3×10^{-5}	6.7×10^{-5}	8.8×10^{-6}	0.0023	1.6×10^{-4}
12.0	12.2	12.1	13.8	12.4

DOI: 10.1021/acs.inorgchem.6b01669
Inorg. Chem. 2016, 55, 12158–12171

metal ions, such as Mn(II), Fe(III), etc., along with strongly axial lanthanides.

■ ASSOCIATED CONTENT

Supporting Information

The Supporting Information is available free of charge on the ACS Publications website at DOI: 10.1021/acs.inorgchem.6b01669.

Details of *ab initio* calculations (PDF)
X-ray crystallographic file in CIF format for **1** (CIF)
X-ray crystallographic file in CIF format for **2** (CIF)
X-ray crystallographic file in CIF format for **3** (CIF)
X-ray crystallographic file in CIF format for **5** (CIF)
X-ray crystallographic file in CIF format for **6** (CIF)

■ AUTHOR INFORMATION

Corresponding Authors

*E-mail: marius.andruh@dnt.ro.
*E-mail: Liviu.Chibotaru@chem.kuleuven.be.

ORCID

Jean-Pascal Sutter: 0000-0003-4960-0579

Notes

The authors declare no competing financial interest.

■ ACKNOWLEDGMENTS

V.V. and L.U. acknowledge the postdoctoral fellowship of Fonds Wetenschappelijk Onderzoek—Vlaanderen (FWO, Flemish Science Foundation). E.S. acknowledges RFBR (Project 16-33-00675 mol_a). Financial support from CNCSIS (PNII-IDEI-912/2009) is gratefully acknowledged.

■ DEDICATION

This paper is dedicated to Professor Ionel Haiduc, on the occasion of his 80th birthday.

■ REFERENCES

(1) Sessoli, R.; Gatteschi, D.; Caneschi, A.; Novak, M. A. Magnetic bistability in a metal-ion cluster. *Nature* **1993**, *365*, 141.

(2) (a) Leuenberger, M. N.; Loss, D. Quantum computing in molecular magnets. *Nature* **2001**, *410*, 789. (b) Bogani, L.; Wernsdorfer, W. Molecular spintronics using single-molecule magnets. *Nat. Mater.* **2008**, *7*, 179. (c) Timco, G. A.; Carretta, S.; Troiani, F.; Tuna, F.; Pritchard, R. J.; Muryn, C. A.; McInnes, E. J. L.; Ghirri, A.; Candini, A.; Santini, P.; Amoretti, G.; Affronte, M.; Winpenny, R. E. P. Engineering the coupling between molecular spin qubits by coordination chemistry. *Nat. Nanotechnol.* **2009**, *4*, 173. (d) Troiani, F.; Affronte, M. Molecular spins for quantum information technologies. *Chem. Soc. Rev.* **2011**, *40*, 3119. (e) Aromí, G.; Aguilà, D.; Gamez, P.; Luis, F.; Roubeau, O. Design of magnetic coordination complexes for quantum computing. *Chem. Soc. Rev.* **2012**, *41*, 537. (f) Gambardella, P.; Stepanow, S.; Dmitriev, A.; Honolka, J.; de Groot, F. M. F.; Lingenfelder, M.; Gupta, S. S.; Sarma, D. D.; Bencok, P.; Stanescu, S.; Clair, S.; Pons, S.; Lin, N.; Seitsonen, A. P.; Brune, H.; Barth, J. V.; Kern, K. Supramolecular control of the magnetic anisotropy in two-dimensional high-spin Fe arrays at a metal interface. *Nat. Mater.* **2009**, *8*, 189.

(3) (a) Friedman, J. R.; Sarachik, M. P.; Tejada, J.; Ziolo, R. Macroscopic Measurement of Resonant Magnetization Tunneling in High-Spin Molecules. *Phys. Rev. Lett.* **1996**, *76*, 3830. (b) Caciuffo, R.; Amoretti, G.; Murani, A.; Sessoli, R.; Caneschi, A.; Gatteschi, D. Neutron Spectroscopy for the Magnetic Anisotropy of Molecular Clusters. *Phys. Rev. Lett.* **1998**, *81*, 4744. (c) Christou, G.; Gatteschi, D.; Hendrickson, D. N.; Sessoli, R. Single-Molecule Magnets. *MRS Bull.* **2000**, *25*, 66. (d) Gatteschi, D.; Sessoli, R.; Cornia, A. Single-molecule magnets based on iron(III) oxo clusters. *Chem. Commun.* **2000**, 725. (e) Gatteschi, D.; Sessoli, R. Quantum Tunneling of Magnetization and Related Phenomena in Molecular Materials. *Angew. Chem., Int. Ed.* **2003**, *42*, 268. (f) Aromí, G.; Brechin, E. K. Synthesis of 3d Metallic Single-Molecule Magnets. *Struct. Bonding (Berlin)* **2006**, *122*, 1. (g) Song, Y.; Zhang, P.; Ren, X.−M.; Shen, X.−F.; Li, Y.−Z.; You, X.−Z. Octacyanometallate-Based Single-Molecule Magnets: $Co^{II}_9M^{V}_6$ (M = W, Mo). *J. Am. Chem. Soc.* **2005**, *127*, 3708. (h) Gatteschi, D.; Sessoli, R.; Villain, J. *Molecular Nanomagnets*; Oxford University Press: Oxford, U.K., 2006. (i) Milios, C. J.; Vinslava, A.; Wernsdorfer, W.; Moggach, S.; Parsons, S.; Perlepes, S. P.; Christou, G.; Brechin, E. K. A Record Anisotropy Barrier for a Single-Molecule Magnet. *J. Am. Chem. Soc.* **2007**, *129*, 2754. (j) Milios, C. J.; Inglis, R.; Jones, L. F.; Prescimone, A.; Parsons, S.; Wernsdorfer, W.; Brechin, E. K. Constructing clusters with enhanced magnetic properties by assembling and distorting Mn_3 building blocks. *Dalton. Trans.* **2009**, 2812. (k) Milios, C. J.; Winpenny, R. E. P. Cluster-Based Single-Molecule Magnets. *Struct. Bonding (Berlin, Ger.)* **2014**, *164*, 1.

(4) (a) Sangregorio, C.; Ohm, T.; Paulsen, C.; Sessoli, R.; Gatteschi, D. Quantum Tunneling of the Magnetization in an Iron Cluster Nanomagnet. *Phys. Rev. Lett.* **1997**, *78*, 4645. (b) Wernsdorfer, W.; Sessoli, R. Quantum Phase Interference and Parity Effects in Magnetic Molecular Clusters. *Science* **1999**, *284*, 133. (c) Milios, C. J.; Inglis, R.; Bagai, R.; Wernsdorfer, W.; Collins, A.; Moggach, S.; Parsons, S.; Perlepes, S. P.; Christou, G.; Brechin, E. K. Enhancing SMM properties in a family of $[Mn_6]$ clusters. *Chem. Commun.* **2007**, 3476.

(5) Ishikawa, N.; Sugita, M.; Ishikawa, T.; Koshihara, S.; Kaizu, Y. Lanthanide Double-Decker Complexes Functioning as Magnets at the Single-Molecular Level. *J. Am. Chem. Soc.* **2003**, *125*, 8694.

(6) (a) Hewitt, I. J.; Lan, Y.; Anson, C. E.; Luzon, J.; Sessoli, R.; Powell, A. K. Opening up a dysprosium triangle by ligand oximation. *Chem. Commun.* **2009**, 6765. (b) Sessoli, R.; Powell, A. K. Strategies towards single molecule magnets based on lanthanide ions. *Coord. Chem. Rev.* **2009**, *253*, 2328. (c) Woodruff, D. N.; Winpenny, R. E. P.; Layfield, R. A. Lanthanide Single-Molecule Magnets. *Chem. Rev.* **2013**, *113*, 5110. (d) Guo, Y.; Chen, X.; Xue, S.; Tang, J. Modulating Magnetic Dynamics of Three Dy_2 Complexes through Keto−Enol Tautomerism of the o-Vanillin Picolinoylhydrazone Ligand. *Inorg. Chem.* **2011**, *50*, 9705. (e) Xu, G.; Wang, Q.; Gamez, P.; Ma, Y.; Clérac, R.; Tang, J.; Yan, S.; Cheng, P.; Liao, D. A promising new route towards single-molecule magnets based on the oxalate ligand. *Chem. Commun.* **2010**, *46*, 1506. (f) Katoh, K.; Kajiwara, T.; Nakano, M.; Nakazawa, Y.; Wernsdorfer, W.; Ishikawa, N.; Breedlove, B. K.; Yamashita, M. Magnetic Relaxation of Single-Molecule Magnets in an External Magnetic Field: An Ising Dimer of a Terbium(III)−Phthalocyaninate Triple-Decker Complex. *Chem. - Eur. J.* **2011**, *17*, 117. (g) Tian, H.; Zhao, L.; Guo, Y. N.; Guo, Y.; Tang, J.; Liu, Z. Quadruple-CO_3^{2-} bridged octanuclear dysprosium(III) compound showing single-molecule magnet behavior. *Chem. Commun.* **2012**, *48*, 708. (h) Langley, S. K.; Moubaraki, B.; Murray, K. S. Magnetic Properties of Hexanuclear Lanthanide(III) Clusters Incorporating a Central μ_6-Carbonate Ligand Derived from Atmospheric CO_2 Fixation. *Inorg. Chem.* **2012**, *51*, 3947. (i) Woodruff, D. N.; Tuna, F.; Bodensteiner, M.; Winpenny, R. E. P.; Layfield, R. A. Single-Molecule Magnetism in Tetrametallic Terbium and Dysprosium Thiolate Cages. *Organometallics* **2013**, *32*, 1224. (j) Pointillart, F.; Le Guennic, B.; Golhen, S.; Cador, O.; Maury, O.; Ouahab, L. A redox-active luminescent ytterbium based single molecule magnet. *Chem. Commun.* **2013**, *49*, 615. (k) Morita, T.; Katoh, K.; Breedlove, B. K.; Yamashita, M. Controlling the Dipole−Dipole Interactions between Terbium(III) Phthalocyaninato Triple-Decker Moieties through Spatial Control Using a Fused Phthalocyaninato Ligand. *Inorg. Chem.* **2013**, *52*, 13555. (l) Zhang, P.; Zhang, L.; Tang, J. Lanthanide single molecule magnets: progress and perspective. *Dalton Trans.* **2015**, *44*, 3923. (m) Layfield, R.; Murugesu, M. *Lanthanides and Actinides in Molecular Magnetism*; Wiley-VCH: 2015.

(7) (a) Ungur, L.; Chibotaru, L. F. Magnetic anisotropy in the excited states of low symmetry lanthanide complexes. *Phys. Chem. Chem. Phys.* **2011**, *13*, 20086. (b) Watanabe, A.; Yamashita, A.; Nakano, M.;

DOI: 10.1021/acs.inorgchem.6b01669
Inorg. Chem. 2016, 55, 12158−12171

Yamamura, T.; Kajiwara, T. Multi-Path Magnetic Relaxation of Mono-Dysprosium(III) Single-Molecule Magnet with Extremely High Barrier. *Chem. - Eur. J.* **2011**, *17*, 7428. (c) Singh, S. K.; Gupta, T.; Shanmugam, M.; Rajaraman, G. Unprecedented magnetic relaxation via the fourth excited state in low-coordinate lanthanide single-ion magnets: a theoretical perspective. *Chem. Commun.* **2014**, *50*, 15513. (d) Blagg, R. J.; Ungur, L.; Tuna, F.; Speak, J.; Comar, P.; Collison, D.; Wernsdorfer, W.; McInnes, E. J. L.; Chibotaru, L. F.; Winpenny, R. E. P. Magnetic relaxation pathways in lanthanide single-molecule magnets. *Nat. Chem.* **2013**, *5*, 673. (e) Guo, Y.−N.; Ungur, L.; Granroth, G. E.; Powell, A. K.; Wu, C.; Nagler, S. E.; Tang, J.; Chibotaru, L. F.; Cui, D. An NCN-pincer ligand dysprosium single-ion magnet showing magnetic relaxation via the second excited state. *Sci. Rep.* **2014**, *4*, 5471.

(8) (a) Guo, Y.−N.; Xu, G.−F.; Wernsdorfer, W.; Ungur, L.; Guo, Y.; Tang, J.; Chibotaru, L. F.; Powell, A. K. Strong Axiality and Ising Exchange Interaction Suppress Zero-Field Tunneling of Magnetization of an Asymmetric Dy_2 Single-Molecule Magnet. *J. Am. Chem. Soc.* **2011**, *133*, 11948. (b) Feltham, H. L. C.; Lan, Y.; Klower, F.; Ungur, L.; Chibotaru, L. F.; Powell, A. K.; Brooker, S. A Non-sandwiched Macrocyclic Monolanthanide Single-Molecule Magnet: The Key Role of Axiality. *Chem. - Eur. J.* **2011**, *17*, 4362. (c) Chibotaru, L. F. Theoretical Understanding of Anisotropy in Molecular Nanomagnets. *Struct. Bonding (Berlin, Ger.)* **2014**, *164*, 185.

(9) (a) Nazari Verani, C.; Weyhermüller, T.; Rentschler, E.; Bill, E.; Chaudhuri, P. A rational assembly of a series of exchange coupled linear heterotrinuclear complexes of the type $M_AM_BM_C$ as exemplified by $Fe^{III}Cu^{II}Ni^{II}$, $Fe^{III}Ni^{II}Cu^{II}$ and $Co^{III}Cu^{II}Ni^{II}$. *Chem. Commun.* **1998**, 2475. (b) Nazari Verani, C.; Rentschler, E.; Weyhermüller, T.; Bill, E.; Chaudhuri, P. Exchange coupling in a bis(heterodinuclear) $[Cu^{II}Ni^{II}]_2$ and a linear heterotrinuclear complex $Co^{III}Cu^{II}Ni^{II}$. Synthesis, structures and properties. *J. Chem. Soc., Dalton Trans.* **2000**, 251. (c) Nazari Verani, C.; Rentschler, E.; Weyhermüller, T.; Bill, E.; Chaudhuri, P. On the rational synthesis and properties of exchange-coupled heterotrinuclear systems containing $[M_AM_BM_B]$ and $[M_AM_BM_C]$ cores. *J. Chem. Soc., Dalton Trans.* **2000**, 4263.

(10) (a) Andruh, M. Oligonuclear complexes as tectons in crystal engineering: structural diversity and magnetic properties. *Chem. Commun.* **2007**, 2565. (b) Andruh, M. Compartmental Schiff-base ligands—a rich library of tectons in designing magnetic and luminescent materials. *Chem. Commun.* **2011**, *47*, 3025.

(11) (a) Visinescu, D.; Sutter, J.-P.; Ruiz-Pérez, C.; Andruh, M. A new synthetic route towards heterotrimetallic complexes. Synthesis, crystal structure and magnetic properties of a $[Cu^{II}Mn^{II}Cr^{III}]$ trinuclear complex. *Inorg. Chim. Acta* **2006**, *359*, 433. (b) Wang, H.; Zhang, L.-F.; Ni, Z.-H.; Zhong, W.-F.; Tian, L.-J.; Jiang, J. Synthesis, Crystal Structures, and Magnetic Properties of One-Dimensional Mixed Cyanide- and Phenolate-Bridged Heterotrimetallic Complexes. *Cryst. Growth Des.* **2010**, *10*, 4231.

(12) (a) Nesterov, D. S.; Kokozay, V. N.; Skelton, B. W. A Pentanuclear Cu/Co/Ni Complex with 2-(Dimethylamino)ethanol − Observation of a Rare Molecular Structure Type and Its Place in General Structural Types: An Analysis of the Cambridge Structural Database. *Eur. J. Inorg. Chem.* **2009**, *2009*, 5469. (b) Nesterov, D. S.; Graiff, C.; Tiripicchio, A.; Pombeiro, A. J. L. Direct synthesis and crystal structure of a new pentanuclear heterotrimetallic Cu/Co/Ni complex with 2-(dimethylamino)ethanol. Discussion of possible "butterfly-like" molecular structure types. *CrystEngComm* **2011**, *13*, 5348.

(13) (a) Gheorghe, R.; Andruh, M.; Costes, J.-P.; Donnadieu, B. A rational synthetic route leading to 3d−3d′−4f heterospin systems: self-assembly processes involving heterobinuclear 3d−4f complexes and hexacyanometallates. *Chem. Commun.* **2003**, 2778. (b) Gheorghe, R.; Cucos, P.; Andruh, M.; Costes, J.-P.; Donnadieu, B.; Shova, S. Oligonuclear 3d−4f Complexes as Tectons in Designing Supramolecular Solid-State Architectures: Impact of the Nature of Linkers on the Structural Diversity. *Chem. - Eur. J.* **2006**, *12*, 187. (c) Sun, W.-B.; Yan, P.-F.; Li, G.-M.; Zhang, J.-W.; Gao, T.; Suda, M.; Einaga, Y. One-dimensional salen-type heterospin trimetallic (3d−4f−3d′) chain-like coordination polymers: Syntheses, crystal structures and magnetic properties. *Inorg. Chem. Commun.* **2010**, *13*, 171. (d) Gao, T.; Yan, P.-F.; Li, G.-M.; Zhang, J.-W.; Sun, W.-B.; Suda, M.; Einaga, Y. Correlations between structure and magnetism of three *N,N′*-ethylene-bis(3-methoxysalicylideneimine) gadolinium complexes. *Solid State Sci.* **2010**, *12*, 597. (e) Gheorghe, R.; Madalan, A. M.; Costes, J.-P.; Wernsdorfer, W.; Andruh, M. A heterotrimetallic 3d−3d′−4f single chain magnet constructed from anisotropic high-spin 3d−4f nodes and paramagnetic spacers. *Dalton Trans.* **2010**, *39*, 4734. (f) Chen, C.; Liu, Y.; Li, P.; Zhou, H.; Shen, X. Construction of $Ni^{II}Ln^{III}M^{III}$ (Ln = Gd^{III}, Tb^{III}; M = Fe^{III}, Cr^{III}) clusters showing slow magnetic relaxations. *Dalton Trans.* **2015**, *44*, 20193. (g) Zhou, H.; Chen, C.; Liu, Y.; Shen, X. Construction of copper(II)−dysprosium(III)−iron(III) trinuclear cluster based on Schiff base ligand: Synthesis, structure and magnetism. *Inorg. Chim. Acta* **2015**, *437*, 188. (h) Hu, K.-Q.; Jiang, X.; Wu, S.-Q.; Liu, C.-M.; Cui, A.-L.; Kou, H.-Z. Slow Magnetization Relaxation in $Ni^{II}Dy^{III}Fe^{III}$ Molecular Cycles. *Inorg. Chem.* **2015**, *54*, 1206. (i) Ding, D.-D.; Gao, T.; Sun, O.; Li, G.-M.; Wu, Y.-H.; Xu, M.-M.; Zou, X.-Y.; Yan, P.-F. Heteropolynuclear Schiff-base complexes Cu−Ln−Fe (Ln = Sm & Pr) with magnetic property. *Inorg. Chem. Commun.* **2015**, *51*, 21. (j) Yao, M.-X.; Zheng, Q.; Qian, K.; Song, Y.; Gao, S.; Zuo, J.-L. Controlled Synthesis of Heterotrimetallic Single-Chain Magnets from Anisotropic High-Spin 3d−4f Nodes and Paramagnetic Spacers. *Chem. - Eur. J.* **2013**, *19*, 294.

(14) (a) Visinescu, D.; Madalan, A. M.; Andruh, M.; Duhayon, C.; Sutter, J.-P.; Ungur, L.; Van den Heuvel, W.; Chibotaru, L. F. First Heterotrimetallic {3d-4d-4f} Single Chain Magnet, Constructed from Anisotropic High-Spin Heterometallic Nodes and Paramagnetic Spacers. *Chem. - Eur. J.* **2009**, *15*, 11808. (b) Visinescu, D.; Jeon, I.-R.; Madalan, A. M.; Alexandru, M.-G.; Jurca, B.; Mathonière, C.; Clérac, R.; Andruh, M. Self-assembly of $[Cu^{II}Tb^{III}]^{3+}$ and $[W(CN)_8]^{3-}$ tectons: a case study of a mixture containing two complexes showing slow-relaxation of the magnetization. *Dalton Trans.* **2012**, *41*, 13578. (c) Dhers, S.; Feltham, H. L. C.; Clérac, R.; Brooker, S. Design of One-Dimensional Coordination Networks from a Macrocyclic {3d-4f} Single-Molecule Magnet Precursor Linked by $[W(CN)_8]^{3-}$ Anions. *Inorg. Chem.* **2013**, *52*, 13685. (d) Bridonneau, N.; Chamoreau, L.-M.; Lainé, P. P.; Wernsdorfer, W.; Marvaud, V. A new versatile class of hetero-tetra-metallic assemblies: highlighting single-molecule magnet behavior. *Chem. Commun.* **2013**, *49*, 9476. (e) Song, X.-J.; Zhang, Z.-C.; Xu, Y.-L.; Wang, J.; Zhou, H.-B.; Song, Y. Assembling 1D magnetic chain based on octacyanotungstate(V) and $[Cu_2L_2Ln]$ sub-building units (Ln = Eu, Gd, Tb and Dy). *Dalton Trans.* **2013**, *42*, 9505. (f) Palacios, M. A.; Mota, A. J.; Ruiz, J.; Hänninen, M. M.; Sillanpää, R.; Colacio, E. Diphenoxo-Bridged $Ni^{II}Ln^{III}$ Dinuclear Complexes as Platforms for Heterotrimetallic $(Ln^{III}Ni^{II})_2Ru^{III}$ Systems with a High-Magnetic-Moment Ground State: Synthesis, Structure, and Magnetic Properties. *Inorg. Chem.* **2012**, *51*, 7010. (g) Alexandru, M.-G.; Visinescu, D.; Madalan, A. M.; Lloret, F.; Julve, M.; Andruh, M. $[W(bipy)(CN)_6]^-$: A Suitable Metalloligand in the Design of Heterotrimetallic Complexes. The First $Cu^{II}Ln^{III}W^{V}$ Trinuclear Complexes. *Inorg. Chem.* **2012**, *51*, 4906. (h) Alexandru, M.-G.; Visinescu, D.; Shova, S.; Lloret, F.; Julve, M.; Andruh, M. Two-Dimensional Coordination Polymers Constructed by $[Ni^{II}Ln^{III}]$ Nodes and $[W^{IV}(bpy)(CN)_6]^{2-}$ Spacers: A Network of $[Ni^{II}Dy^{III}]$ Single Molecule Magnets. *Inorg. Chem.* **2013**, *52*, 11627.

(15) Shiga, T.; Okawa, H.; Kitagawa, S.; Ohba, M. Stepwise Synthesis and Magnetic Control of Trimetallic Magnets $[Co_2Ln(L)_2(H_2O)_4]$-$[Cr(CN)_6]\cdot nH_2O$ (Ln = La, Gd; H_2L = 2,6-Di(acetoacetyl)pyridine) with 3-D Pillared-Layer Structure. *J. Am. Chem. Soc.* **2006**, *128*, 16426.

(16) (a) Sutter, J.-P.; Dhers, S.; Rajamani, R.; Ramasesha, S.; Costes, J.-P.; Duhayon, C.; Vendier, L. Hetero-Metallic {3d-4f-5d} Complexes: Preparation and Magnetic Behavior of Trinuclear $[(LMe_2Ni-Ln)\{W(CN)_8\}]$ Compounds (Ln = Gd, Tb, Dy, Ho, Er, Y; LMe_2 = Schiff base) and Variable SMM Characteristics for the Tb Derivative. *Inorg. Chem.* **2009**, *48*, 5820. (b) Dhers, S.; Sahoo, S.; Costes, J.-P.; Duhayon, C.; Ramasesha, S.; Sutter, J.-P. 1-D hydrogen-bonded organization of hexanuclear {3d-4f-5d} complexes: evidence for slow relaxation of the magnetization for $[\{LMe_2Ni(H_2O)Ln(H_2O)_{4.5}\}_2\{W(CN)_8\}_2]$ with Ln

DOI: 10.1021/acs.inorgchem.6b01669
Inorg. Chem. 2016, 55, 12158−12171

= Tb and Dy. *CrystEngComm* **2009**, *11*, 2078. (c) Dhers, S.; Costes, J.-P.; Guionneau, P.; Paulsen, C.; Vendier, L.; Sutter, J.-P. On the importance of ferromagnetic exchange between transition metals in field-free SMMs: examples of ring-shaped hetero-trimetallic $[(LnNi_2)\{W(CN)_8\}]_2$ compounds. *Chem. Commun.* **2015**, *51*, 7875.

(17) Visinescu, D.; Desplanches, C.; Imaz, I.; Bahers, V.; Pradhan, R.; Villamena, F.; Guionneau, P.; Sutter, J.-P. Evidence for Increased Exchange Interactions with 5d Compared to 4d Metal Ions. Experimental and Theoretical Insights into the Ferromagnetic Interactions of a Series of Trinuclear $[\{M(CN)_8\}^{3-}/Ni^{II}]$ Compounds (M = Mo^V or W^V). *J. Am. Chem. Soc.* **2006**, *128*, 10202.

(18) (a) Pasatoiu, T. D.; Sutter, J.-P.; Madalan, A. M.; Fellah, F. Z. C.; Duhayon, C.; Andruh, M. Preparation, Crystal Structures, and Magnetic Features for a Series of Dinuclear $[Ni^{II}Ln^{III}]$ Schiff-Base Complexes: Evidence for Slow Relaxation of the Magnetization for the Dy^{III} Derivative. *Inorg. Chem.* **2011**, *50*, 5890. (b) Khuntia, P.; Mariani, M.; Mahajan, A. V.; Lascialfari, A.; Borsa, F.; Pasatoiu, T. D.; Andruh, M. Magnetic properties and spin dynamics of 3d−4f molecular complexes. *Phys. Rev. B: Condens. Matter Mater. Phys.* **2011**, *84*, 184439.

(19) (a) Pasatoiu, T. D.; Etienne, M.; Madalan, A. M.; Andruh, M.; Sessoli, R. Dimers and chains of {3d−4f} single molecule magnets constructed from heterobimetallic tectons. *Dalton Trans.* **2010**, *39*, 4802. (b) Pasatoiu, T. D.; Ghirri, A.; Madalan, A. M.; Affronte, M.; Andruh, M. Octanuclear $[Ni^{II}_4Ln^{III}_4]$ complexes. Synthesis, crystal structures and magnetocaloric properties. *Dalton Trans.* **2014**, *43*, 9136. (c) Pasatoiu, T. D.; Etienne, M.; Madalan, A. M.; Sessoli, R.; Andruh, M. Crystal structures and magnetic properties of two new heterodinuclear $[Ni^{II}Ln^{III}]$ complexes obtained using a side-off compartmental ligand and 2,6-pirydin-dicarboxylato coligand. *Rev. Roum. Chim.* **2012**, *57*, 507.

(20) Dennis, C. R.; Van Wyk, A. J.; Basson, S. S.; Leipoldt, J. G. Synthesis of cesium octacyanomolybdate(V)- and cesium octacyanotungstate(V) dihydrate: a more successful method. *Transition Met. Chem.* **1992**, *17*, 471.

(21) (a) Aquilante, F.; De Vico, L.; Ferré, N.; Ghigo, G.; Malmqvist, P.-Å.; Neogrády, P.; Pedersen, T. B.; Pitoňák, M.; Reiher, M.; Roos, B. O.; Serrano-Andrés, L.; Urban, M.; Veryazov, V.; Lindh, R. MOLCAS 7: The Next Generation. *J. Comput. Chem.* **2010**, *31*, 224. (b) Chibotaru, L. F.; Ungur, L.; Aronica, C.; Elmoll, H.; Pilet, G.; Luneau, D. Structure, Magnetism, and Theoretical Study of a Mixed-Valence $Co^{II}_3Co^{III}_4$ Heptanuclear Wheel: Lack of SMM Behavior despite Negative Magnetic Anisotropy. *J. Am. Chem. Soc.* **2008**, *130*, 12445.

(22) Seijo, L.; Barandiarán, Z.*Computational Chemistry: Reviews of Current Trends*; Leszczynski, J., Ed.; World Scientific: Singapore, 1999; Vol. *4*, p 55.

(23) Andersson, K.; Roos, B. O. Excitation energies in the nickel atom studied with the complete active space SCF method and second-order perturbation theory. *Chem. Phys. Lett.* **1992**, *191*, 507.

(24) http://molcas.org/documentation/manual/.

(25) Lines, M. E. Orbital Angular Momentum in the Theory of Paramagnetic Clusters. *J. Chem. Phys.* **1971**, *55*, 2977.

(26) (a) Chibotaru, L. F.; Ungur, L.; Soncini, A. The Origin of Nonmagnetic Kramers Doublets in the Ground State of Dysprosium Triangles: Evidence for a Toroidal Magnetic Moment. *Angew. Chem., Int. Ed.* **2008**, *47*, 4126. (b) Ungur, L.; Van den Heuvel, W.; Chibotaru, L. F. *Ab initio* investigation of the non-collinear magnetic structure and the lowest magnetic excitations in dysprosium triangles. *New J. Chem.* **2009**, *33*, 1224.

(27) Neese, F. The ORCA program system. *Wiley Interdiscip. Rev.: Comput. Mol. Sci.* **2012**, *2*, 73.

(28) Rodriguéz-Dieguéz, A.; Kivekäs, R.; Sillanpää, R.; Cano, J.; Lloret, F.; McKee, V.; Stoeckli-Evans, H.; Colacio, E. Structural and Magnetic Diversity in Cyano-Bridged Bi- and Trimetallic Complexes Assembled from Cyanometalates and $[M(rac\text{-}CTH)]^{n+}$ Building Blocks (CTH = d,l-5,5,7,12,12,14-Hexamethyl-1,4,8,11-tetraazacyclotetradecane). *Inorg. Chem.* **2006**, *45*, 10537.

(29) Griffith, J. S. *The Theory of Transition-Metal Ions*; Cambridge University Press: Cambridge, U.K., 1971.

(30) Kramers, H. A. Théorie générale de la rotation paramagnétique dans les cristaux. *Proc. Amsterdam Acad.* **1930**, *33*, 959.

(31) Griffith, J. S. Spin Hamiltonian for Even-Electron Systems Having Even Multiplicity. *Phys. Rev.* **1963**, *132*, 316.

(32) Yamaguchi, K.; Takahara, Y.; Fueno, T. In *Applied Quantum Chemistry*; Smith, V. H., Jr., Schaefer, H. F., III, Morokuma, K., Eds.; Springer: Dordrecht, 1986; p 155.

(33) Chibotaru, L. F.; Mironov, V. S.; Ceulemans, A. Origin of Ferromagnetism in Cyano-Bridged Compounds Containing d^1 Octacyanometallates. *Angew. Chem., Int. Ed.* **2001**, *40*, 4429.

(34) Goodenough, J. B. Theory of the Role of Covalence in the Perovskite-Type Manganites [La, M(II)]MnO_3. *Phys. Rev.* **1955**, *100*, 564.

(35) Podgajny, R.; Pełka, R.; Desplanches, C.; Ducasse, L.; Nitek, W.; Korzeniak, T.; Stefańczyk, O.; Rams, M.; Sieklucka, B.; Verdaguer, M. W-Knotted Chain $\{[Cu^{II}(dien)]_4[W^V(CN)_8]\}^{5+}_{\infty}$: Synthesis, Crystal Structure, Magnetism, and Theory. *Inorg. Chem.* **2011**, *50*, 3213.

(36) Ungur, L.; Thewissen, M.; Costes, J.-P.; Wernsdorfer, W.; Chibotaru, L. F. Interplay of Strongly Anisotropic Metal Ions in Magnetic Blocking of Complexes. *Inorg. Chem.* **2013**, *52*, 6328.

DOI: 10.1021/acs.inorgchem.6b01669
Inorg. Chem. 2016, 55, 12158−12171